

Faculdade de Engenharia da Universidade do Porto



BESO - Battery Energy Storage Optimization

Miguel Francisco Ruivo Loureiro

Dissertation submitted in partial fulfilment of the requirements for the
Degree of Master of Science in Electrical and Computers Engineering

Supervisor: Vladimiro Miranda (Full Professor)

Jan 2020

Resumo

Este trabalho apresenta um modelo para apoiar o processo de tomada de decisão de investimento da perspectiva de um fornecedor de energia independente que deseja integrar sistemas de baterias em redes de distribuição. Para apoiar a decisão, um conjunto condicional de soluções ótimas economicamente viáveis para o modelo de negócio de compra e venda de energia é identificado, a fim de permitir que outros critérios de decisão (por exemplo, redução de perdas, confiabilidade, serviços auxiliares etc.) possam ser avaliados para aprimorar os benefícios econômicos como resultado das sinergias entre diferentes aplicações dos sistemas de baterias. Para isso, um novo modelo de otimização baseado na utilização de uma meta-heurística, Differential Evolutionary Particle Swarm Optimization (DEEPSO) e redes neurais Group Method of Data Handling (GMDH) é proposto para dimensionamento, localização e operação dos sistemas de baterias. Os resultados obtidos indicam que, após identificar o custo de break-even do modelo de negócio, é possível obter uma boa qualidade no conjunto de decisão condicional para avaliar outras alternativas de negócios.

Abstract

This paper presents a model for supporting the investment decision-making process from the perspective of an independent energy provider that wants to integrate batteries in distribution networks. For supporting the decision, a conditional set of optimal solutions economically viable for the business model of buying and selling energy is identified in order to allow other decision criteria (e.g. loss reduction, reliability, ancillary services, etc.) to be evaluated to enhance the economic benefits as results of the synergies between different applications of BESS. For this purpose, a novel approach optimization model based on the metaheuristic Differential Evolutionary Particle Swarm Optimization (DEEPSO) and Group Data Method Handling (GMDH) neural networks is proposed for sizing, location, and Battery Energy Storage systems (BESS) operation schedule. The results obtained indicate that after identifying the breakeven cost of the business model, a good quality of conditional decision set can be obtained for assessing then other business alternatives.

Acknowledgements

Firstly, I would like to thank Professor Vladimiro Miranda for the opportunity to work on a very interesting and challenging topic, as well as for his valuable advice and guidance.

I would also like to thank INESC TEC for welcoming me into their offices and opportunity to work in stimulating environment.

Many thanks to Tiago and Piedy for all the time and dedication spent in the development of this work.

Thank you to my friends who accompanied me at this stage of my academic life, particularly Pedro and João for the daily companionship and Luis for the willingness to help.

Finally, I would like to thank my family and Loreto for their patience and words of encouragement.

Table of Contents

Resumo	iii
Abstract	v
Acknowledgements.....	vii
Table of Contents.....	ix
List of Figures	xi
List of Tables	xiv
Abbreviations.....	xv
Chapter 1.....	1
Introduction	1
Chapter 2.....	4
State of the Art	4
2.1. Battery Energy Storage Systems	4
2.2. Applications of Energy Storage Systems	11
2.3. Energy Markets.....	13
2.4. GMDH.....	16
2.5. Metaheuristics.....	18
Chapter 3.....	23
Stochastic Scenarios	23
3.1. Scenarios Generation	23
Chapter 4.....	27
DEEPSO application for sizing and location	27
4.1. Sizing and Location.....	28
4.2. Battery Operation	30
Chapter 5.....	34
Numerical experiments and validation	34
5.1. CIGRE MV Distribution Network benchmark.....	34
5.2. Stochastic Scenario Creation.....	36
5.3. Business model experiments	38

5.4. Methods Validation.....	49
Chapter 6.....	54
Conclusions and Future Work.....	54
6.1. Conclusions.....	54
6.2. Future work	55
References	56

List of Figures

Figure 2-1 - Battery discharging (left) and charging (right)	5
Figure 2-2 - Development of specific energy and energy density with respect to cost per watt-hour of Li-ion batteries	6
Figure 2-3 - Redox Flow battery	8
Figure 2-4 - Supercapacitor scheme	9
Figure 2-5 - Flywheel scheme.....	10
Figure 2-6 - Schematic of time-shifting of energy	12
Figure 2-7 - Example of daily market.....	15
Figure 2-8 - Neuron model	16
Figure 2-9 -Formation of network's layers.....	17
Figure 2-10 -Eliminating worst r indices in each layer (Red) and finding the best r index in the last layer (Green)	17
Figure 2-11 -Final formation of a GMDH network.....	18
Figure 2-12 - Illustrating the movement of a particle, influenced by three terms	19
Figure 2-13 - EPSO scheme	20
Figure 3-1 - Daily load curve formation	24
Figure 3-2 - Seasonal weather conditions probability	24
Figure 3-3 - Scheme of the season selection process.....	25
Figure 3-4 - Scheme of the weather selection process.....	25
Figure 3-5 - Stochastic scenario creation	26
Figure 4-1 - Proposed methodology scheme	28
Figure 4-2 - Proposed particle structure	28
Figure 4-3 - BESS cost components.....	29

Figure 4-4 - MATLAB/GAMS information exchange	31
Figure 4-5 - Proposed GMDH architecture	32
Figure 4-6 - Proposed methodology's flowchart	33
Figure 5-1 - Topology of the CIGRE MV Distribution network benchmark - European configuration	35
Figure 5-2 - Load in Bus 5 over 10 days	36
Figure 5-3 - Load in bus 5 over 6 months	36
Figure 5-4 - PV Generation in bus 5 over 10 days.	37
Figure 5-5 - Energy prices over 10 days.....	37
Figure 5-6 -Battery operation (down) relative to energy price (up) over 1 day.....	40
Figure 5-7 - Battery operation (down) relative to energy price (up) over 5 days.....	40
Figure 5-8 - Examples of solutions for the very optimistic scenario that compound the conditional decision set.....	41
Figure 5-9 - Examples of solutions for the optimistic scenario that compound the conditional decision set.....	41
Figure 5-10 - Examples of solutions for the break-even scenario that compound the conditional decision set.....	41
Figure 5-11 - 5% step of dispersion histogram of the results of solutions for the very optimistic scenario.	42
Figure 5-12 - 5% step of dispersion histogram of the results of solutions for the optimistic scenario.	43
Figure 5-13 - 5% step of dispersion histogram of the results of solutions for the break-even scenario.	43
Figure 5-14 - - Battery operation (down) relative to energy price (up) over 1 day.....	45
Figure 5-15 - - Battery operation (down) relative to energy price (up) over 5 days	46
Figure 5-16 - Examples of solutions for the very optimistic scenario that compound the conditional decision set.....	47
Figure 5-17 - Examples of solutions for the optimistic scenario that compound the conditional decision set.....	47
Figure 5-18 - Solution for the break-even scenario that compound the conditional decision set	47
Figure 5-19 - 5% step of dispersion histogram of the results of solution for the very optimistic scenario.	48
Figure 5-20 - 5% step of dispersion histogram of the results of solution for the optimistic scenario.	48

Figure 5-21 - 5% step of dispersion histogram of the results of solutions for the break-even scenario.	49
Figure 5-22 - Comparison of the evolution of the cost best particle found by DEEPSO using just LP (GAMS) or using LP and GMDH (GMDH) for the very optimistic scenario, simulation 1.....	50
Figure 5-23 - Comparison of the evolution of the cost best particle found by DEEPSO using just LP (GAMS) or using LP and GMDH (GMDH) for the very optimistic scenario, simulation 2.....	50
Figure 5-24 - Comparison of the evolution of the cost best particle found by DEEPSO using just LP (GAMS) or using LP and GMDH (GMDH) for the optimistic scenario	52
Figure 5-25 - Comparison of the evolution of the cost best particle found by DEEPSO using just LP (GAMS) or using LP and GMDH (GMDH) for the break-even scenario.....	52

List of Tables

Table 2.1 - Typical values of lead-acid batteries characteristics	5
Table 2.2 - Typical values of nickel-cadmium batteries characteristics	6
Table 2.3 - Typical values of lithium-ion batteries characteristics	7
Table 2.4 - Typical values of Sodium-Sulphur batteries characteristics	7
Table 2.5 - Typical values of zinc-bromine batteries characteristics	8
Table 2.6 - Typical values of vanadium-redox batteries characteristics	9
Table 2.7 - Typical values of supercapacitors characteristics	10
Table 2.8 - Typical values of supercapacitors characteristics	11
Table 5.1 - Capital investment scenario definition	39

Abbreviations

List of abbreviations

AGC	Automatic Generation Control
BESS	Battery Energy Storage System
ESS	Energy Storage System
EPSO	Evolutionary Particle Swarm Optimization
ES	Evolutionary Strategies
GMDH	Group Method of Data Handling
LP	Linear Programming
MSE	Mean Squared Error
OPF	Optimal Power Flow
PSO	Particle Swarm Optimization
PV	Photovoltaic
RES	Renewable Energy Sources
TSO	Transmission System Operator

Chapter 1

Introduction

During the last decades, severe structural changes have been introduced to the distribution and transmission networks due to the challenges imposed by the increase in energy demand, the need of electrification and/or interconnection of new areas, the need of a better integration of the growing share of renewable energy sources (RES), and other technical requirements of the networks, as well as environmental policies or proposals related to the decarbonization. Nowadays, with the accelerated growth, the technical maturity achieved and the diverse technological offer, energy storage systems (ESS) have attracted the attention of electric power systems and have positioned themselves as a technological solution that can offer both technical, economic, and environmental benefit [1],[2]. ESS can convert, through an external interface, electrical energy into a form of storable energy to convert it back into electrical energy and deliver it to distribution or transmission systems when necessary or economically interesting.

ESS, when integrated into the distribution and transmission network, are characterized by several potential applications [1],[3],[4]: power quality improvement; reliability improvement; voltage support; load levelling and peak shaving; load shifting; energy arbitrage; ancillary services; network expansion deferral and support to RES integration and operation.

Despite these numerous and varied applications, the investment costs required by the ESS still have been one of the main barriers towards achieving their massive proliferation [5],[6]. Likewise, for implementing some of these applications, regulatory modifications are still required to guarantee the economic viability of these implementations in the short-term. For mitigating the impact and justifying investment costs, improving the technical benefits offered and its profitability, ESS applications are usually oriented by establishing synergies between these applications [4],[5].

2 Introduction

The technical and economic benefits to be obtained as a result of synergies between applications are significantly related to their optimal sizing and location. In other words, considering the existing barriers due to investment costs and current regulatory frameworks, recent years researches have addressed the problem of integrating ESS in the distribution and transmission network to an optimization problem that aims to find the optimal location for the ESS and/or power, energy capacity and its operation schedule over time [4].

This dissertation proposes a model for supporting the investment decision-making process from the perspective of an independent energy provider that wants to assess business alternatives for integrating BESS in the distribution networks with existing dispersed Photovoltaic (PV) generation. To achieve this goal, a hybrid novel model approach optimization based on a Monte-Carlo approach implemented with the metaheuristic, Differential Evolutionary Particle Swarm Optimization (DEEPSO) and Group Data Method Handling (GMDH) neural networks is proposed. This model controls the process via a DEEPSO procedure for sizing and location of the dispersed BESS and adopts a Linear Programming (LP) formulation for defining the battery operation and training a GMDH neural network for evaluating the battery operation over time.

Chapter 2

State of the Art

2.1. Battery Energy Storage Systems

Battery energy storage systems (BESS) are a type of technology used for energy storage, where chemical energy is stored and converted to electrical energy through electrochemical reactions. There is a wide variety of battery solutions available, however, a great distinction is made between classical batteries and flow batteries [7]. In classical batteries, there is no physical separation between energy conversion unit and active material, while in flow batteries the energy conversion unit and active material are separate. The choice of adequate BESS will depend upon application requirements, such as power and energy rating, size, response time and operating temperature [3].

2.1.1. Classical batteries

Classical batteries are composed of several electrochemical cells. Each cell is composed of a positive (anode) and a negative electrode (cathode) separated by an electrolyte [3]. When a battery discharges through a connected load, electrochemical reactions occur at the two electrodes generating a flow of electrons from anode to cathode. The battery can be charged, by applying an external voltage across the electrodes, reversing the flow of electrons, Figure 2-1 [8].

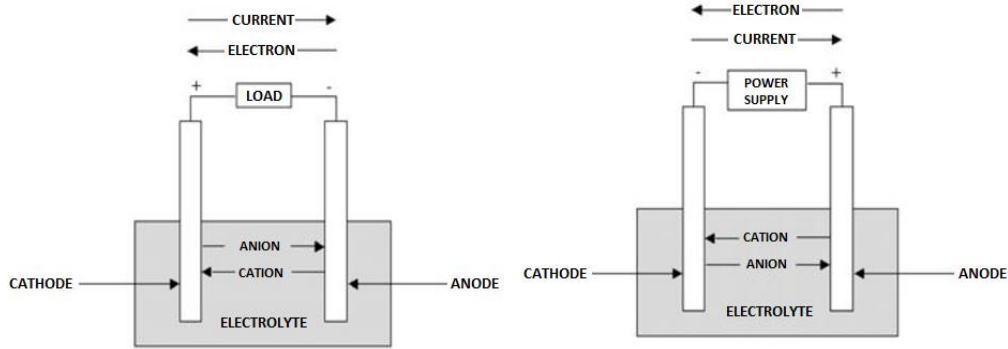


Figure 2-1 - Battery discharging (left) and charging (right) [9]

2.1.1.1. Lead-Acid Battery

This type of battery is the oldest and most commonly used worldwide. They are made of lead plates immersed in an electrolyte solution of sulfuric acid and water. In order to discharge, lead on the cathode and lead dioxide on the anode combine with sulfuric acid present in the electrolyte forming lead sulfate and releasing electrons [10].

Despite being comparatively big and bulky, they are easy to install and have low capital and maintenance costs, as well as high efficiency [3],[8],[11]. Nevertheless, the battery capacity tends to diminish considerably over many charge-discharge cycles, presenting a low life cycle (number of cycles that result in a battery capacity lower than 80% of the initial value) for applications that demand a large depth of discharge. Other limitations include limited energy density and the fact that the toxicity of lead represents an environmental hazard restricting possible applications, despite the possibility of an effective recycling process [12] [13]

Table 2.1 - Typical values of lead-acid batteries characteristics [3][8][14]

Specific energy (Wh/kg)	Specific power (W/kg)	Cycle life	Charge/discharge energy efficiency
25-50	75-300	500-1500	63-90%

2.1.1.2. Nickel-Cadmium Battery

Just like the lead-acid battery, the nickel-cadmium battery (NiCd) is a very mature system. NiCd batteries are constituted by a nickel hydroxide anode, a cadmium hydroxide cathode, a separator, and an alkaline electrolyte.

They have a high energy density, along with good reliability and low maintenance needs [8].

The main downside is the use of cadmium, a highly toxic metal, presents environmental hazards that require careful monitoring of the battery's disposal. This has led to their

prohibition for consumer use and limited to stationary applications in some countries [15] [16]. For this reason, this technology has generally been replaced by Nickel-metal hydride (NiMh) batteries, which additionally possess better energy density and increased cycle life [17]. Their main limitations are high self-discharge rate, and cell rupture risk when charged at a very high rate.

Table 2.2 - Typical values of nickel-cadmium batteries characteristics [3][8][14]

Specific energy (Wh/kg)	Specific power (W/kg)	Cycle life	Charge/discharge energy efficiency
40-75	150-300	2000-2500	70-90%

2.1.1.3. Lithium-Ion Battery

In the last few years, Lithium-Ion batteries have become the fastest-growing technology for stationary storage applications. It is the standard technology for electric vehicles and most consumer electronics, becoming widely commercially available despite being a recent technology when compared to lead-acid batteries [12].

In a lithium-ion battery, the cathode is a lithiated metal, the anode is made of graphitic carbon with a layering structure and the electrolyte is made up of lithium salts dissolved in organic carbonates [8].

This technology has very high efficiency, a high energy density and cycle life (as high as 10,000 cycles) as well as a low self-discharge rate. The main limitation of this technology is its high cost [11]. Nonetheless, with its rise in popularity, there was a significant decrease in the cost with respect to the increase in specific energy and energy density, resulting in lower material required for the manufacturing as represented in Figure 2-2.

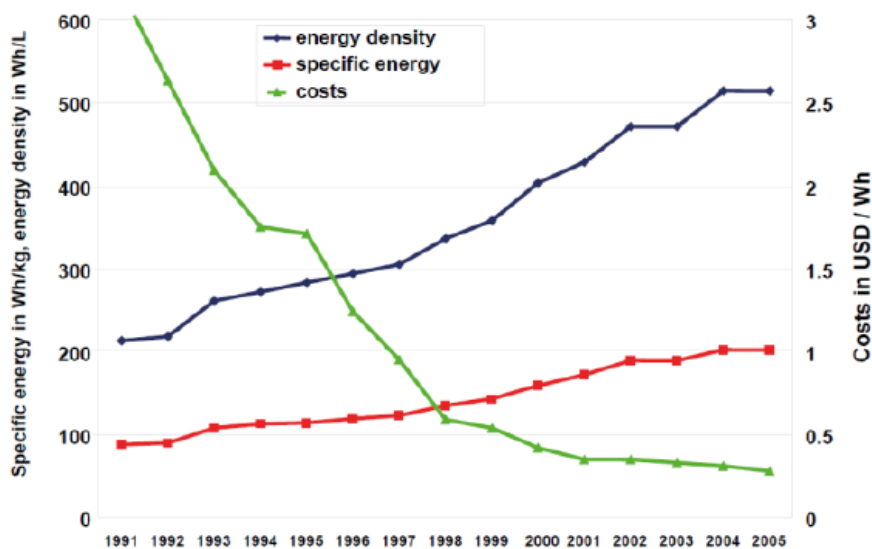


Figure 2-2 - Development of specific energy and energy density with respect to cost per watt-hour of Li-ion batteries [3]

Table 2.3 - Typical values of lithium-ion batteries characteristics [3][8][14]

Specific energy (Wh/kg)	Specific power (W/kg)	Cycle life	Charge/discharge energy efficiency
150-300	200-315	1000-10000+	95%

2.1.1.4. Sodium-Sulphur Battery

Sodium-sulphur batteries consist of a molten sulphur cathode and molten sodium anode, separated by a solid beta alumina ceramic electrolyte [18].

This technology holds its potential mainly for energy applications due to its long discharge capabilities and presents a high cycle life [12]. However, the operating temperature should be kept between 270°C and 350°C, which requires a heat source that partially reduces the battery’s performance.

Table 2.4 - Typical values of Sodium-Sulphur batteries characteristics [3][8][14]

Specific energy (Wh/kg)	Specific power (W/kg)	Cycle life	Charge/discharge energy efficiency
150-300	90-230	2500-5000	75-90%

2.1.2. Flow batteries

Flow batteries are a form of battery that converts electrical energy into chemical potential energy by means of a reversible electrochemical reaction between two liquid electrolyte solutions [19]. Contrary to classical batteries, flow batteries store energy in the electrolyte solutions and, therefore, the power and energy ratings are independent, with the storage capacity determined by the quantity of electrolyte used and the power rating determined by the active area of the cell stack.

Generally, a flow battery is made up of several electrochemical cells. Each cell stores two electrolytes separated by an ion-exchange membrane. Two tanks are used to store the electrolytes which are then pumped through the cell stack, where the electrolytes will be subject to an oxidation-reduction reaction, as can be seen in Figure 2-3.

This type of batteries varies in consideration to the different electrolytes used, the most common ones include zinc-bromine batteries and vanadium redox batteries.

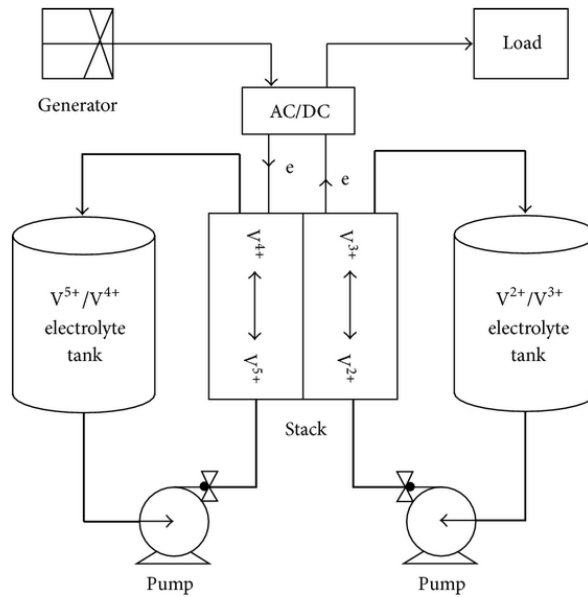


Figure 2-3 - Redox Flow battery [20]

2.1.2.1. Zinc-bromine Batteries

In zinc bromide batteries both electrolytes are from an aqueous zinc bromide solution but with different bromide concentrations. During charge, zinc solidifies and is plated onto the negative electrode. Similarly, bromine is formed at the positive electrode. The cell electrodes are made of carbon plastic and are designed so that a given electrode can serve both as the cathode for one cell and anode for the next cell, also referred as bipolar [12].

Zinc-bromine batteries are suitable for a variety of applications, having discharge times ranging from seconds to several hours [19] which allows them to be both effective for power and energy applications. Further advantages include good specific energy and efficiency.

Table 2.5 - Typical values of zinc-bromine batteries characteristics [8][21]

Specific energy (Wh/kg)	Specific power (W/kg)	Cycle life	Charge/discharge energy efficiency
30-50	-	2000	60-85%

2.1.2.2. Vanadium Redox Batteries

In vanadium redox batteries the electrolyte, commonly constituted by vanadium sulphate dissolved in a solution of mild sulphuric acid [8], is used to store energy from charged ions of

different valence states [3]. Its charging and discharging operation is similar to zinc bromide batteries but with the process using only the ionic forms of vanadium.

Self-discharge is not a problem in this type of flow batteries since electrolytes are stored in separate tanks. Moreover, they have a long cycle life as the active materials do not degrade over time.

Due to their relatively low specific energy, this type of battery is best suited for power applications such as power quality and peak shaving, as energy applications would require large volumes of electrolyte [8].

Table 2.6 - Typical values of vanadium-redox batteries characteristics [3][8][22]

Specific energy (Wh/kg)	Specific power (W/kg)	Cycle life	Charge/discharge energy efficiency
10-30	-	12000+	90-95%

2.1.3. Supercapacitors

Supercapacitors store electrical charge in an electric double layer at the interface between two electrodes with a very large surface area and a liquid electrolyte [7]. While regular capacitors have capacities in the mili-Farad range, supercapacitors have capacities in the kilo-Farad range. They are like regular capacitors in the sense that they are basically double-layered versions of normal capacitors, but with a higher electrode surface area and a fluid electrolyte, Figure 2-4. When a current is applied, dissociate ions in the electrolyte are accumulated on the surface of each electrode, this way an electric charge is stored [22].

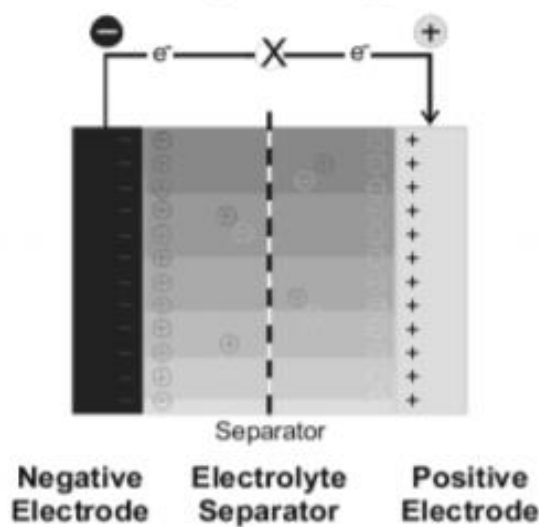


Figure 2-4 - Supercapacitor scheme [23]

Relative to batteries, these have a very high specific power but low energy density [7]. Furthermore, supercapacitors are very durable, with a long cycle life, mainly due to the absence of chemical reactions in the electrodes. They also have a very high efficiency (95%), as well as very fast charge and discharge capabilities. The biggest drawback is the self-discharge rate (around 5% per day), which doesn't allow for long term storage.

Table 2.7 - Typical values of supercapacitors characteristics [3][7][24].

Specific energy (Wh/kg)	Specific power (W/kg)	Cycle life	Charge/discharge energy efficiency
8	10000-20000	10000+	95%

2.1.4. Flywheels

Flywheels are a type of mechanical energy storage, storing energy in the angular momentum of a spinning mass. In order to charge the flywheel, a motor spins its rotor storing kinetic energy, and in order to discharge the same motor acts as a generator producing energy from said kinetic energy [8], as presented in Figure 2-5.

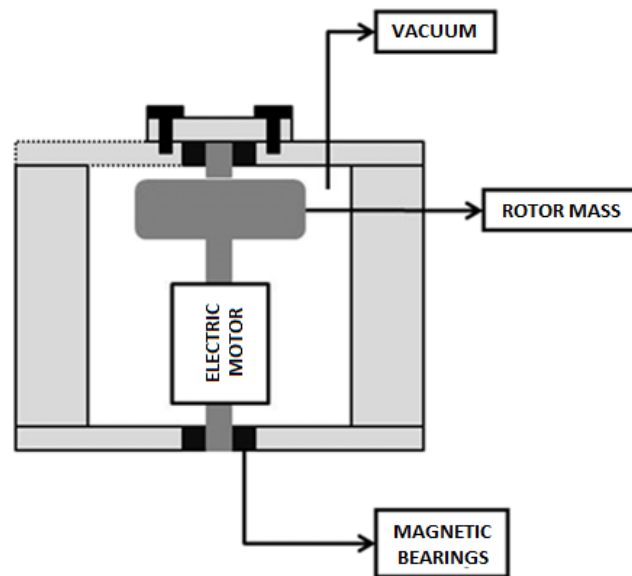


Figure 2-5 - Flywheel scheme

They have a long cycle life capable of providing over 100,000 cycles. However, due to high friction losses causing a high self-discharge rate, long term-storage with this technology is not foreseeable [22]. This, added to its high specific power, makes its use is usually reserved power quality devices.

Table 2.8 - Typical values of supercapacitors characteristics [3][12][25]

Specific energy (Wh/kg)	Specific power (W/kg)	Cycle life	Charge/discharge energy efficiency
5-200	400-30000	100000+	70-96%

2.2. Applications of Energy Storage Systems

Energy storage allows many applications with benefits to the network. These applications are usually categorized relative to their timescale. Firstly, energy applications, when the time scale is larger and large amounts of energy are supplied or absorbed from the grid. Thus, energy applications typically involve long charge or discharge cycles which require the storage system to be scaled to a high storage capacity (MWh). Secondly, power applications, when the time scale is shorter where network stability support is provided. These applications involve injecting active and reactive power over a short period of time, typically seconds to minutes, in order to maintain network stability [26].

2.2.1. Energy Time shift

Time-shifting refers to storing energy in periods of low demand and injecting this energy into periods of high demand, as represented in Figure 2-6. Since prices at low demand times are lower than prices at high demand times this option has the potential to be economically attractive. With the increased integration of RES in the grid, production during off-peak hours can be higher than demand, leading to energy curtailment [12]. This is far from ideal, either economically or environmentally, but can be avoided with the use of ESS to store excess energy and discharging it during peak hours.

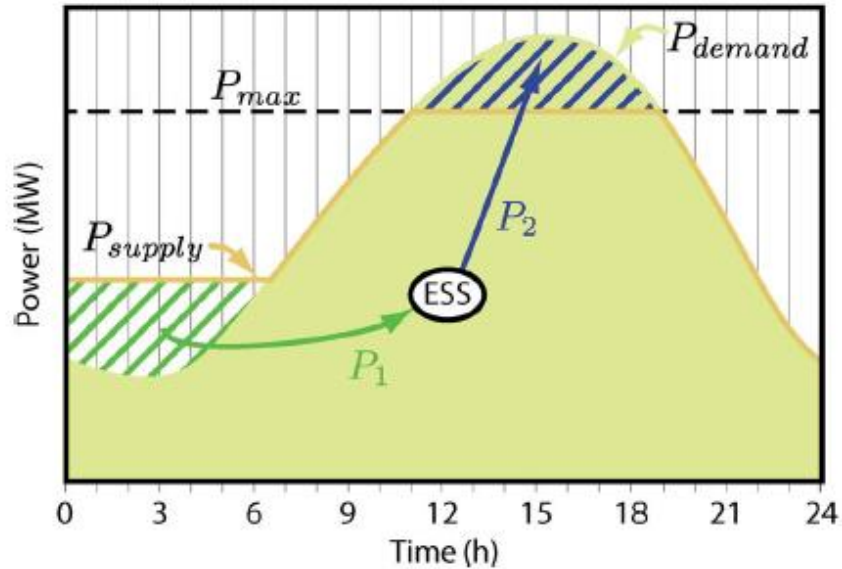


Figure 2-6 - Schematic of time-shifting of energy

Nevertheless, with the increase of energy storage in the grid, the amplitude of prices in the energy market may be reduced, which will in turn, reduce the profitability of energy time-shifting.

2.2.2. Distribution upgrade deferral

ESS allow the postponing or avoiding of investments that would otherwise be required to provide adequate distribution capacity [12].

With ESS it is possible to charge the system during periods of low demand and consume this energy during periods of peak consumption. Therefore, the need to draw electricity from power plants is diminished, which is translated in a reduction of losses and congestion of lines in the distribution grid. This allows postponing investment in the grid infrastructure [21].

2.2.3. Ancillary services

Ancillary services can be defined as all the services required to enable the integrity and stability of the transmission or distribution system, as well as the power quality [27]. ESS enables, among others, the following ancillary services [28]:

1. Frequency control
2. Voltage control
3. Black start capability

2.2.3.1. Frequency Control:

In the electricity grid, demand and supply of energy must be equal during all times in order to maintain the system frequency. Charging ESS can increase demand and discharging can increase supply. We can distinguish three kinds of frequency control:

- i. Primary frequency control: This control is automatic and decentralized and should be activated within a few seconds after an incident provoking a frequency deviation.
- ii. Secondary frequency control: This control is automatic and centralized. The Automatic Generation Control (AGC) controls secondary control power. Its objective is to restore system frequency to its set-point value and to restore power interchange with neighbouring control areas.
- iii. Tertiary control: Controlled by the Transmission System Operator (TSO), it is used to restore the primary and secondary frequency control reserves.

2.2.3.2. Voltage control

The increasing penetration level of RES can cause an increase in distributed networks voltage profiles [29]. Since voltage levels must be within specified limits, their value must be controlled by injection or absorption of reactive power [7]. For this one normally uses systems made for this reason, however, the power components used in storage systems allow its operation to be at a non-unity power factor, in order to supply and absorb reactive power, which permits this function to be performed by an ESS in addition to its primary purpose [17].

2.2.3.3. Black start capability

Under normal operating conditions, most synchronous generators start-up resorting to energy from the grid [30]. However, in the event of system failure that leads to a blackout, this is not possible and the power plants capable of starting up without power from the grid are used to re-energize the other generators. ESS can be used to provide the power and energy necessary to restart other generation units [7],[28]. This would represent another source of revenue through the ancillary services market but, nonetheless, would limit the range of state-of-charge that the battery would be able to operate.

2.3. Energy Markets

Electricity contracting involves multiple forms, from contracting to the next day (daily market), to longer terms (forward market) or bilaterally or through specific legal or regulatory

mechanisms. The following points will refer to the Portuguese market. The Iberian Electric Energy Market (MIBEL) results from the union of the electrical systems of Portugal and Spain.

In MIBEL, energy can be contracted through the following main markets:

- Bilateral contracting market
- Markets managed by the Iberian market operator (OMI):
 - Daily market
 - Intraday market
 - Forward market

There are also ancillary services markets that are separate in Portugal and Spain. Each of the countries is subdivided into several balance areas in order to allow the monitoring of the values of generation and demand. The ancillary services markets are managed by the System Operators of each control area, REN being responsible for its management and operation in Portugal, and REE in Spain. These entities define the required levels and contract, assuming themselves as sole purchasers in the market.

2.3.1. Bilateral Contracting market

Contracts are permitted between all types of producers and other qualified agents, and the conditions under which traders and producers may sell previously acquired energy to other producers or external agents are well established [31].

2.3.2. Daily Market

The configuration of this market is that of a daily market for next-day power delivery, in a format similar to most of those in Europe. Its basic features will be the independent trading of energy for each of the 24-hour periods of the day following its realization. Sales proposals are sorted by price, and purchase proposals are sorted by decreasing order. The market price for each period is obtained by crossing the supply and purchase curves, which is the lowest of the prices that ensures supply meets demand, as illustrated in Figure 2-7.

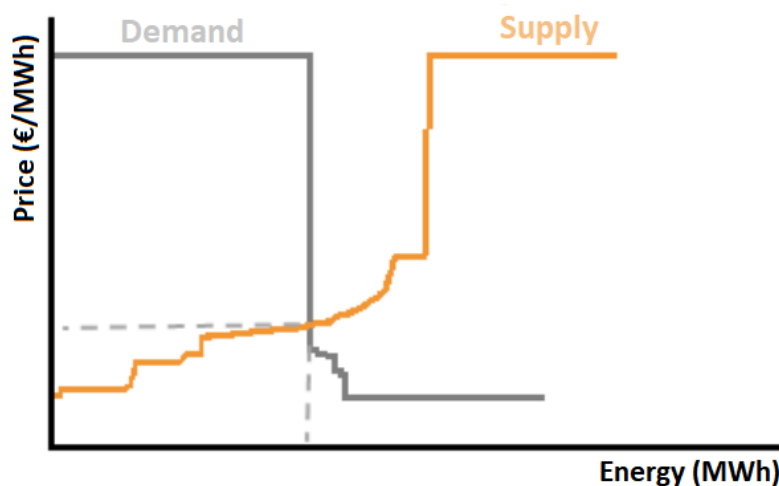


Figure 2-7 - Example of daily market

Congestion resolution uses market splitting mechanisms, which consists of the separation of the market into two price areas in the event of capacity constraints on interconnection [31],[32].

2.3.3. Ancillary Services Market

The system services market deals with the contracting of products separated from the power generation activity related to the safety and reliability of the operation of the electric system. Unlike the rest of these markets, they are separated in Spain and Portugal.

BESS could have a great potential aptitude for this service, and according to the Portuguese market, could have a business opportunity whether in the secondary reserve market as well as in the tertiary reserve market. In the secondary reserve market, the players offer a power regulation band in MW and a price in € / MW. The ratio of upward reserve to downward reserve offered must be of 2/3. In this market, if the player offer is accepted, his price offer will be paid regardless of being the reserve being activated, however, if the reserve is used, the energy will be paid at the value of the tertiary reserve. In the tertiary reserve market, players will bid both upward reserve and downward reserve and a price in € / MWh. This price will only be paid if the reserve is used.

2.4. GMDH

The GMDH [33],[34],[35],[36],[37], is a feed-forward neural network with supervised learning. This type of neuronal network allows the approximation of inputs and outputs with a polynomial function.

For the development of the network, it is necessary to form a training set and a test set defined with n inputs x and an output z . The inputs of the variables are combined two by two, forming a neuron represented by (Eq. 2.1).

$$Y_{ik} = A_{ik} + B_{ik} \cdot x_i + C_{ik} \cdot x_j + D_{ik} \cdot x_i^2 + E_{ik} \cdot x_j^2 + F_{ik} \cdot x_i \cdot x_j \quad (\text{Eq. 2.1})$$

Equation (Eq. 2.1) can be solved by the least-squares method in order to find the coefficients that best fit the training set.

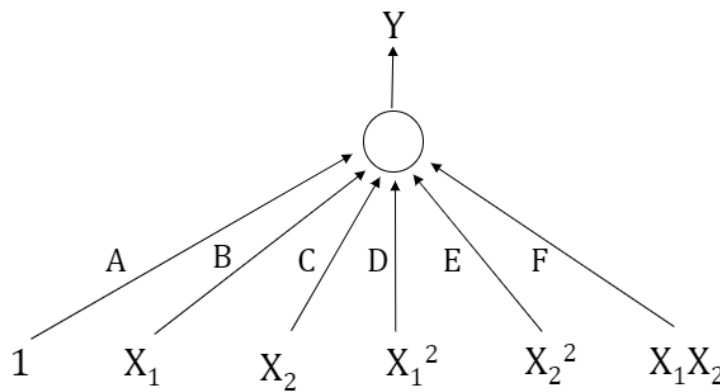


Figure 2-8 - Neuron model

The quality of each neuron is assessed by calculating its Mean Squared Error (MSE) as in (Eq. 2.2):

$$r_{ik}^2 = \frac{\sum_{m=1}^{N_{test}} (y_{ik,m} - z_m)^2}{\sum_{m=1}^{N_{test}} (y_{ik,m})^2} \quad (\text{Eq. 2.2})$$

Neurons can be ordered from r minimum to maximum, thus discriminating the neurons that allow a better approximation between the input-output relationship present in the training data. At this stage, the worst neurons can be eliminated to avoid exponential growth of the network size.

Having assembled the first layer, its outputs should be used as the variables to create a new layer. This process can be repeated until the best r index in a layer is worse than the best of the previous layer.

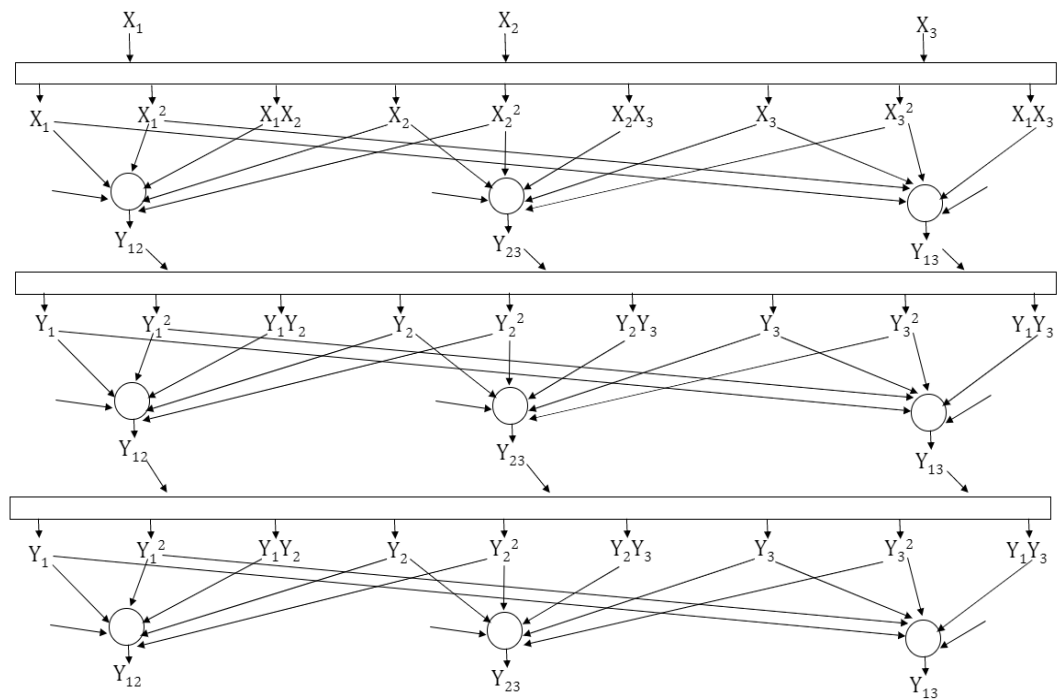


Figure 2-9 -Formation of network's layers

At this moment one can reconstruct a polynomial input-output relation from the created network. For this purpose, the best neuron of the last layer is selected and all neurons which are out of paths between it and the inputs are eliminated, as shown in Figure 2-10 and Figure 2-11.

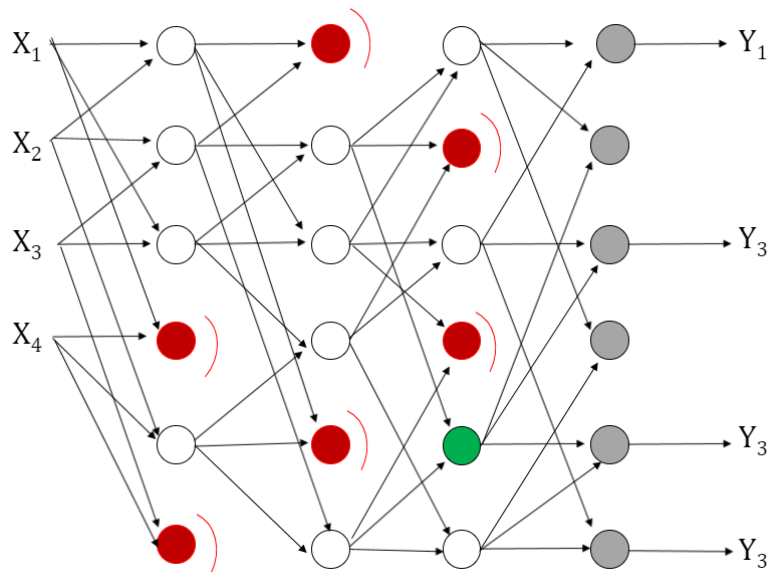


Figure 2-10 -Eliminating worst r indices in each layer (Red) and finding the best r index in the last layer (Green)

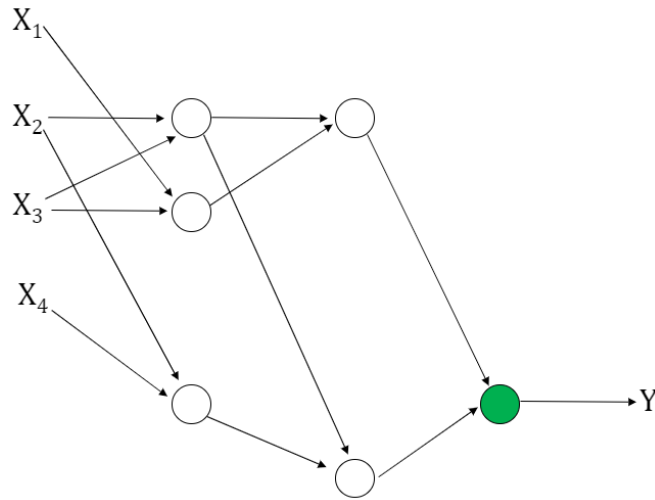


Figure 2-11 -Final formation of a GMDH network

2.5. Metaheuristics

Metaheuristics are general algorithmic frameworks, often inspired in nature, which can be applied to different optimization problems. They are particularly useful in addressing problems that include in their mathematical formulation uncertain, stochastic, and dynamic information [38]. In power systems optimizations, metaheuristics are particularly useful for planning and operation-based problems.

2.5.1. PSO

Particle Swarm Optimization (PSO) [39] relies on mimicking the collective or social behaviour of animal swarms or flocks. It is, therefore, a population-based optimization algorithm, with each population being a set of possible solutions represented by “particles” placed in the space defined by a problem or function. These particles are evaluated by an objective function that ranks them in relation to their fitness.

New particles are formed from an ancestor, according to the *movement rule*, (Eq. 2.3).

$$X_i^{new} = X_i + V_i^{new} \quad (\text{Eq. 2.3})$$

Where V_i^{new} is the particle i velocity, defined by (Eq. 2.4):

$$V_i^{new} = Dec(t) \cdot w_{i0} \cdot V_i + Rnd_1 \cdot w_{i1} \cdot (b_i - X_i) + Rnd_2 \cdot w_{i2} \cdot (b_g - X_i) \quad (\text{Eq. 2.4})$$

This equation can be decomposed in three terms, as represented in Figure 2-12 and as follows:

- The first term represents Inertia, meaning each particle is inclined to move in the direction it was previously moving.
- The second term expresses memory, this is, each particle is attracted to the past best, promoting the particle to search the most promising region visited in its lifetime.
- Finally, the third term represents cooperation, the particles are attracted to the best point found by all particles in any generation.

The parameters w_{i1} are weights fixed at the beginning of the process, Rnd_x are numbers sampled randomly by a uniform distribution in $[0, 1]$ and $Dec(t)$ is a function which decreases with the evolution of the iterations, diminishing the influence of inertia.

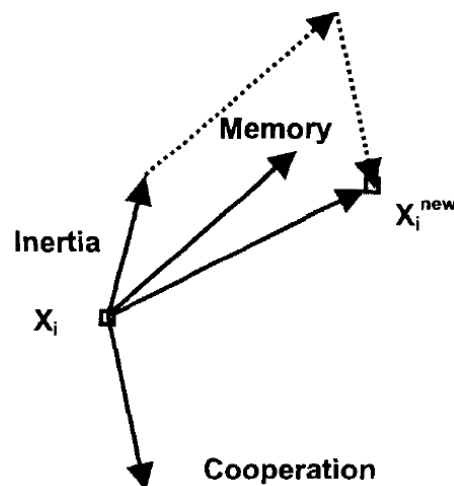


Figure 2-12 - Illustrating the movement of a particle, influenced by three terms [40]

PSO depends on a number of parameters externally defined by a user, and therefore requires an arduous work of fine-tuning the algorithm to obtain optimal results. This drawback is overcome with the method described in the next section.

2.5.2. EPSO

Evolutionary Particle Swarm Optimization (EPSO) [40],[41],[42] is an auto-adaptive evolutionary algorithm. Therefore, it depends on a selection operator and its parameters are not fixed, but instead possess self-adapting properties. This way, this method combines the

benefits of Evolution Strategies (ES), namely the Darwinist process of selection, and PSO, namely the particle movement rule.

The variables used in EPSO formulation are divided into object parameters (the X variables) and strategic parameters (the weights w), each particle is a set of object and strategic parameters [X, w].

A general scheme for EPSO is present in Figure 2-13 and is as follows:

- REPLICATION - each particle is replicated r times;
- MUTATION - each particle has its weights w mutated;
- REPRODUCTION - each mutated particle generates an offspring according to the particle movement rule;
- EVALUATION - each offspring has its fitness evaluated;
- SELECTION - by stochastic tournament or elitist selection, the best particles survive to form a new generation;

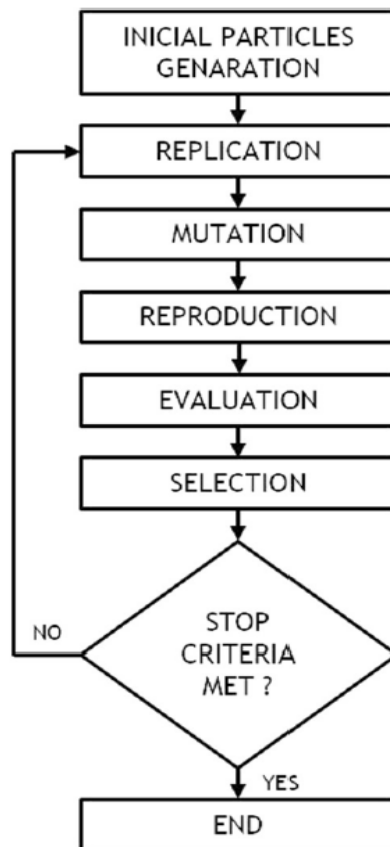


Figure 2-13 - EPSO scheme [43]

The velocity equation is like the one used in PSO, however, as previously mentioned, the weights are mutated as presented in (Eq. 2.5) and (Eq. 2.6). This grants self-adaptive properties to the algorithm by automatically adjusting its parameters in response to the development of the particle's fitness.

$$V_i^{new} = w_{i0}^* \cdot V_i + w_{i1}^* \cdot (b_i - X_i) + C \cdot w_{i2}^* \cdot (b_g - X_i) \quad (\text{Eq. 2.5})$$

$$w_{ik}^* = w_{ik} + \tau \cdot N(0,1) \quad (\text{Eq. 2.6})$$

In (Eq. 2.5), C is a binary variable equal to 1 with a given probability p , and 0 with probability $(1-p)$, used in order to simulate the effects of lack of communication between members of the swarm. (Eq. 2.6) represents a basic additive mutation rule for the weights, however, one can use other mutation strategies such as $w_{ik}^* = w_{ik}[1 + \tau \cdot N(0,1)]$.

The global best can also be disturbed by adding noise to the exact location of b_g , as presented in (Eq 2.7), with beneficial results:

$$b_g^* = b_g + \tau' \cdot N(0,1) \quad (\text{Eq. 2.7})$$

In (Eq. 2.7) τ and τ' are learning parameters and can also be subject to mutation.

2.5.3. DEEPSO

DEEPSO is an advanced version or variant of EPSO, originally developed to incorporate some traits of Differential Evolution. The core of DE lies in a given population of individuals generating a new solution from an existing individual from the sum of fractions obtained by the difference between two sampled points of the population, X_{r1} and X_{r2} .

Similarly, EPSO, in the motion equation, evaluates the macro-gradient of the objective function by the difference between two points, the current position and the best location. This reasoning led to the proposal of a generalization of EPSO, equal to EPSO in sequence, however with a transformation of the movement rule now expressed as (Eq. 2.8):

$$V_i^{new} = w_{i0}^* \cdot V_i + w_{i1}^* \cdot (X_{r1} - X_{r2}) + C \cdot w_{i2}^* \cdot (b_g - X_i) \quad (\text{Eq. 2.8})$$

Due to the dependence on the particle evaluating the macro-gradient of the objective function, in a DEEPSO scheme, in a minimization context, the particles must be ordered such as (Eq. 2.7):

$$f(X_{r1}) < f(X_{r2}) \quad (\text{Eq. 2.9})$$

22 State of the Art

Several variants may be defined, depending on how the particles are sampled: from the current generation set, or sampled from the set of local best particles. Also, note that DEEPSO defines that X_{r_1} is equal to X and only X_{r_2} is sampled [44].

Chapter 3

Stochastic Scenarios

In order to test the proposed methodology, it is necessary to consider a scenario of loads, generation and energy price. For this, a stochastic model was developed from historical data of the Portuguese network. For this, a Monte-Carlo sampling approach is used where uniformly distributed random numbers are used to form the scenarios distribution. For typical load, the data used was gathered from *EDP Distribuição* [45] public records. The photovoltaic generation data was from a PV station situated in Évora, Portugal [46]. Finally, for energy prices, data was gathered from OMIE public records [47]. The resulting scenario, as well as all the data used, is composed of one-hour intervals.

3.1. Scenarios Generation

In order to create the stochastic scenario, the available data were grouped by seasons of the year: Winter, Spring, Summer, and Autumn. For the load data, year-round load forecasting was available for each type of consumer (Residential and Commercial/Industrial). Thus, although each bus contemplates more than one type of consumer, it was possible to join the daily load curves by type of consumer and create a single daily load curve by bus, as presented in Figure 3-1.

24 Stochastic Scenarios

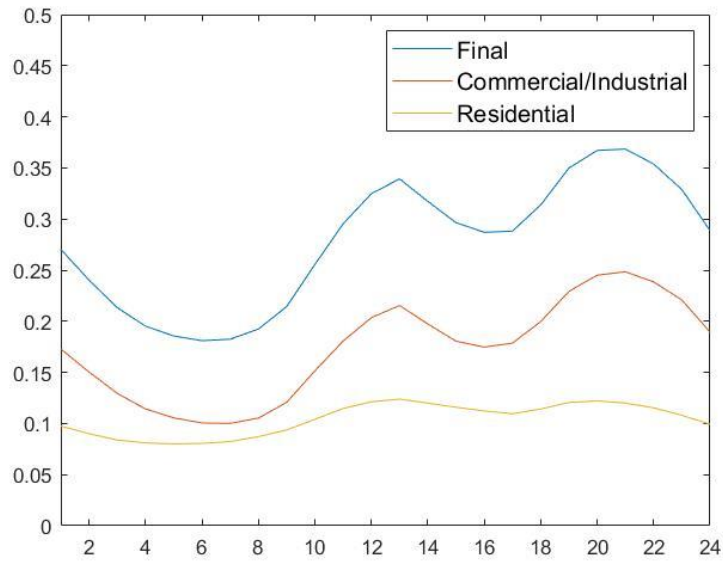


Figure 3-1 - Daily load curve formation

For the PV generation, the average value for each season was used considering the weather conditions. The weather conditions considered have different probabilities of occurring and vary according to the season as presented in Figure 3-2.

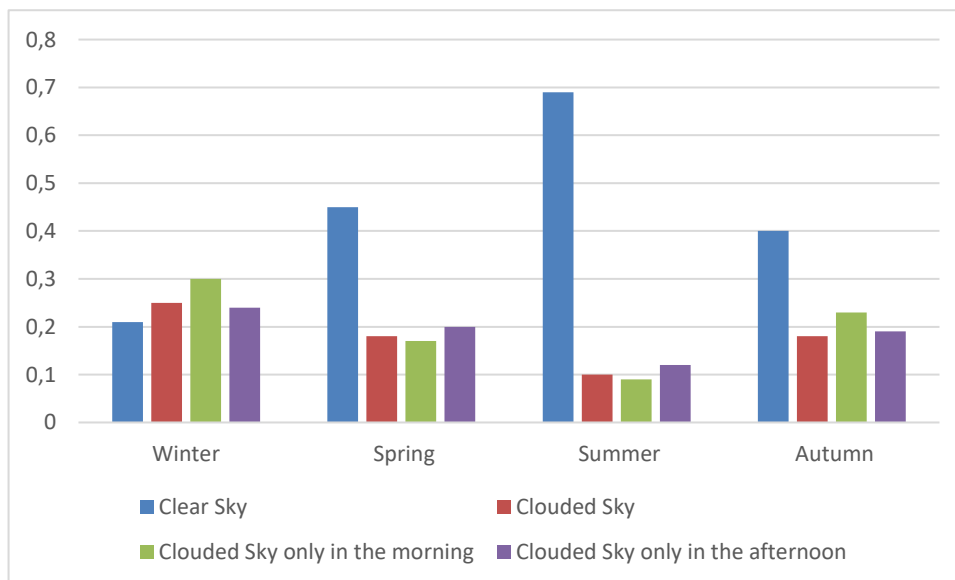


Figure 3-2 - Seasonal weather conditions probability

The energy prices used were 21-day samples of the daily market price curves for each season. For each season, each sample contained 6 weekend days for a better representation of the differences in load patterns on weekdays and weekends.

3.1.1. Day scenario generation

In order to create the stochastic scenario, each day is generated individually. For each day, a random value (α) is drawn between zero and one from a normal distribution. This value defines the season of the year corresponding to the day according to Figure 3-3.

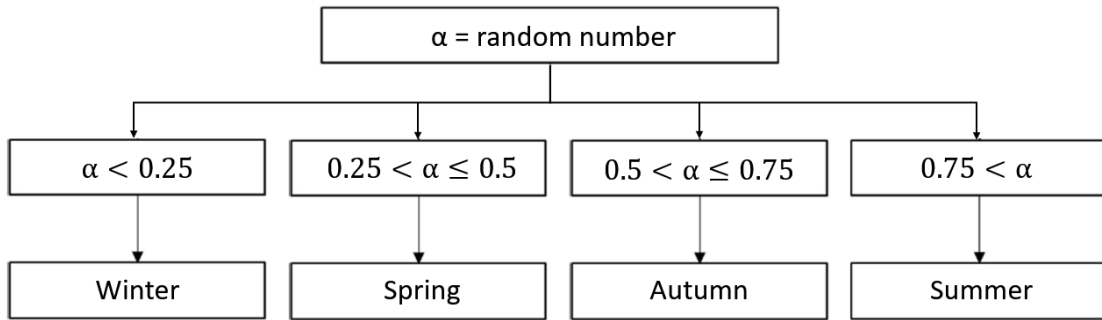


Figure 3-3 - Scheme of the season selection process

Once the season for that day is defined, a random number (β), will be drawn from the total number of days of that season, which will define the daily load curve. For the price curve of that day, yet another random number (γ) is drawn that will select the energy price data of that day from the total number of days corresponding to that season present in the database. To be noted that if the load curve corresponds to a weekend, the price data will also be associated with a weekend, otherwise, the price data will correspond to a weekday.

Finally, the weather condition for that day is selected by a final random value (β), as represented in Figure 3-4. The resulting weather condition and season will define the PV generation daily curve. This is done according to the probabilities defined in Figure 3-2, such that CS is the clear sky probability, CM is the cloudy in the morning probability, CA is the cloudy in the afternoon probability and CD is the cloudy day probability.

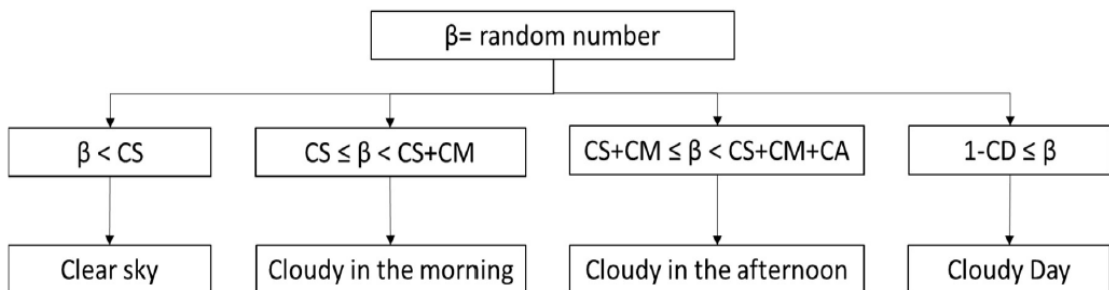


Figure 3-4 - Scheme of the weather selection process

This way load price and PV generation data are saved in the database used in this scenario.

3.1.2. Final scenario

In order to obtain a database with the scenario to be used in the proposed methodology, the process described in Section 3.1.1. is repeated until the desired number of days is obtained, and thus generating a sequential series, stored in a database for load, PV generation and energy price, as can be seen in Figure 3-5.

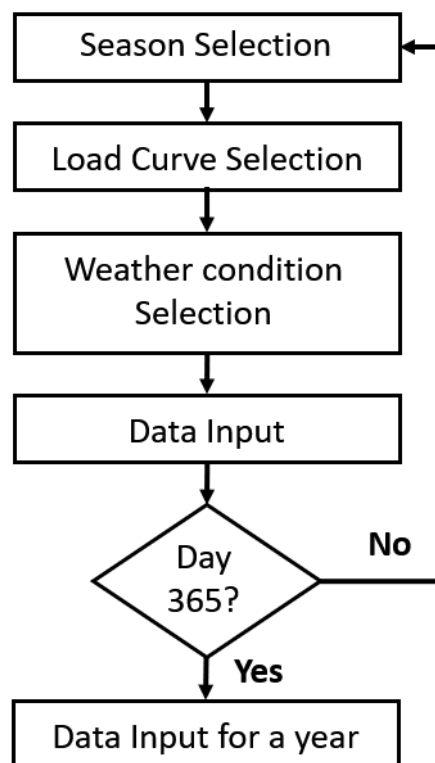


Figure 3-5 - Stochastic scenario creation

With this approach, the database will have a season data dispersed through the year instead of being grouped by season. This differs from a proper global sequential simulation process, guaranteeing a larger sampling dispersion of initial conditions for the simulation of each day, which is performed in a sequential way within 24-hour periods. This allows the generation of a larger sampling data dispersion over what would otherwise be achieved with a classical grouping of season data.

Chapter 4

DEEPSO application for sizing and location

In this chapter the proposed methodology will be presented, as well as the proposed software tool for solving battery sizing and location problems in the distribution network. This problem is composed of two sub-problems. First, at a higher level, the location and sizing of the BESS are calculated using DEEPSO. In the second sub-problem, the operation of each BESS is determined, at first using mathematical programming, and then, after a number of iterations, a GMDH type neural network, which allows to greatly decrease computational time.

Figure 4-1 presents an overview of the proposed methodology. Every iteration, the data of each particle is transmitted to the lower level problem, from which the BESS operation is optimized in order to allow maximum economic gains. The results are then returned to the Upper-level problem.

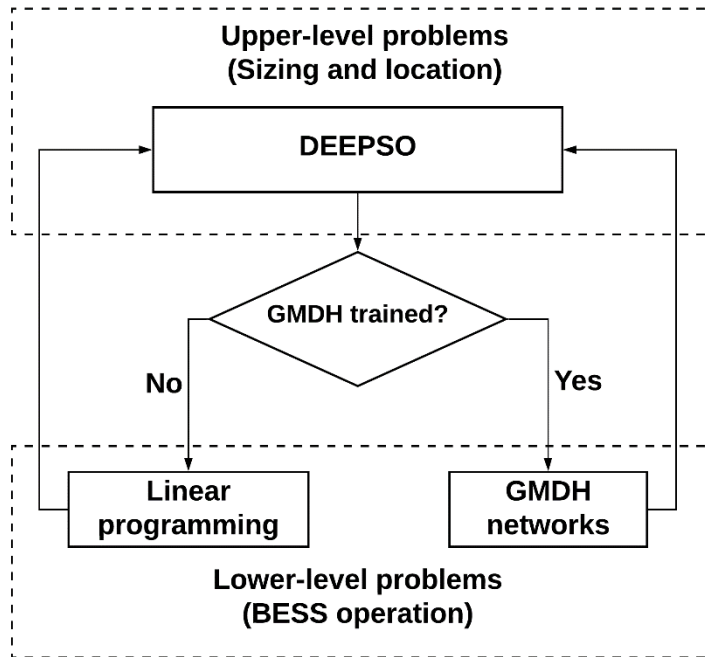


Figure 4-1 - Proposed methodology scheme

4.1. Sizing and Location

For this part of the problem, a MATLAB [48] script was developed. As noted, the location and sizing of batteries in the network is a problem solved by DEEPSO.

In the proposed model each particle represents a possible solution to the sizing and location problem. The objective parameters will be the battery's capacity and its discharge/charge rate. However, there are several possible buses for the location, and therefore, for an N-bus distribution network, a 2N-element particle is created, so that each pair of elements represents, respectively, the battery's capacity and its charging/discharging rate, as represented in Figure 4-2. Thus, the position of that battery on the particle defines the network bus on which it is located.

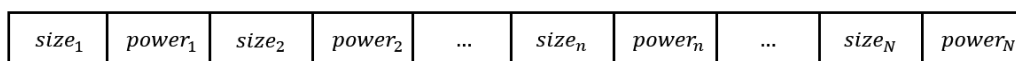


Figure 4-2 - Proposed particle structure

After the generation of the particles of each iteration, it is necessary to evaluate the fitness of each solution. For this purpose, the fitness function described in (Eq. 4.1) considers the operational revenue generated by the battery, the capital investment in energy-related costs

and power-related costs, maintenance costs, and penalties when line power flow limits are violated. The penalties for line power flow limit violations are high in order to prevent those particles that do not comply with the network's operation requirements advance to further iterations.

$$\min Fit = \sum_{n=1}^N Investment + Maintenance - Operation + penalties \quad (\text{Eq. 4.1})$$

As presented in Figure 4-3, regarding the capital cost of a BESS, one must consider the cost of the storage technology, such as the battery pack, as well as its interface with the network. The latter also includes the costs of installing the system and connecting it to the electrical network. Both the energy cost and power cost will be represented by a linear function.

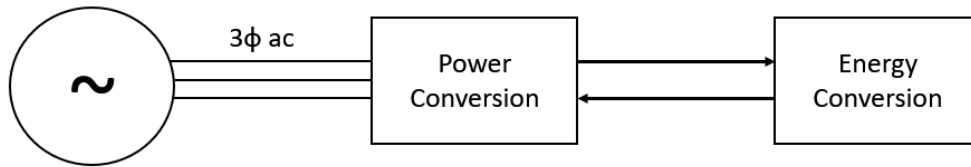


Figure 4-3 - BESS cost components

The capital cost calculation of a BESS can be expressed as (Eq. 4.2):

$$Investment(\text{€/MWh}) = Energy\ Cost(\text{€/MWh}) + Power\ Cost(\text{€/MW}) \quad (\text{Eq. 4.2})$$

For a proper financial analysis, the operational costs should be actualized according to the battery's lifespan.

$$Cost = p \cdot \frac{(1+i)^Y - 1}{i \cdot (1+i)^Y} \quad (\text{Eq. 4.3})$$

In which:

- p - Batteries annual yield (€);
- i - Interest rate (e.g. 8%);
- y - lifespan in years;

The network model considered implements a DC optimal power flow (OPF) to evaluate its performance. The DC OPF allows the simplification of the power flow problem by considering a series of approximations: ignoring reactive power, consider all voltages as one and ignore losses. Thus, the power flow problem can be represented by a series of linear equations that, albeit result in a less accurate model, drastically reduce the computational effort relative to AC OPF.

$$P_{k,t} = \sum_{k=1}^N Pl_{k,t} - \sum_{k=1}^N Pg_{k,t} \quad (\text{Eq. 4.4})$$

$$Pflow_t = A \cdot P_t \quad (\text{Eq. 4.5})$$

$$|Pflow_{ik,t}| \leq Pflow_{ik}^{max} \quad (\text{Eq. 4.6})$$

In which:

- $P_{k,t}$ - Power in bus k on time period t;
- $Pl_{k,t}$ - Load in bus k on time period t;
- $Pg_{k,t}$ - Power generation in bus n on time period t;
- $Pflow_t$ - Power flow matrix in time period t;
- A - Sensitivity matrix;
- $Pflow_{ik,t}$ - Power flow in the line ik;
- $Pflow_{ik}^{max}$ - Maximum power flow in the line ik;

In order to consider the battery's operation, the value charged, $Bl_{k,t}$, or discharged, $Bg_{k,t}$, in each period is represented, respectively, as an increase in load and generation, such as (Eq. 4.7) and (Eq. 4.8). To be noted that $Bl_{k,t}$ and $Bg_{k,t}$ represent only positive values.

$$Pl_{k,t} = Pl_{nB_{k,t}} + Bl_{k,t} \quad (\text{Eq. 4.7})$$

$$Pg_{k,t} = Pg_{nB_{k,t}} + Bg_{k,t} \quad (\text{Eq. 4.8})$$

In which $Pl_{nB_{k,t}}$ and $Pg_{nB_{k,t}}$ represent respectively, the load and generation on bus k and time period t without any implemented battery.

4.2. Battery Operation

4.2.1. Mathematical programming

The operation of a battery in the distribution network must be defined as an optimization problem with a cost function defined by financial benefits, through a metric of network operation benefits or a combination of the two. In this work, the operation of each battery in the distribution network will be optimized by mathematical programming with the objective of maximizing revenue, and with that purpose, a model is developed in GAMS [49].

Therefore, MATLAB is used to handle the input data of the battery operation optimization model and send it to GAMS. Subsequently, GAMS is used to solve the optimization model and the results are sent to MATLAB.

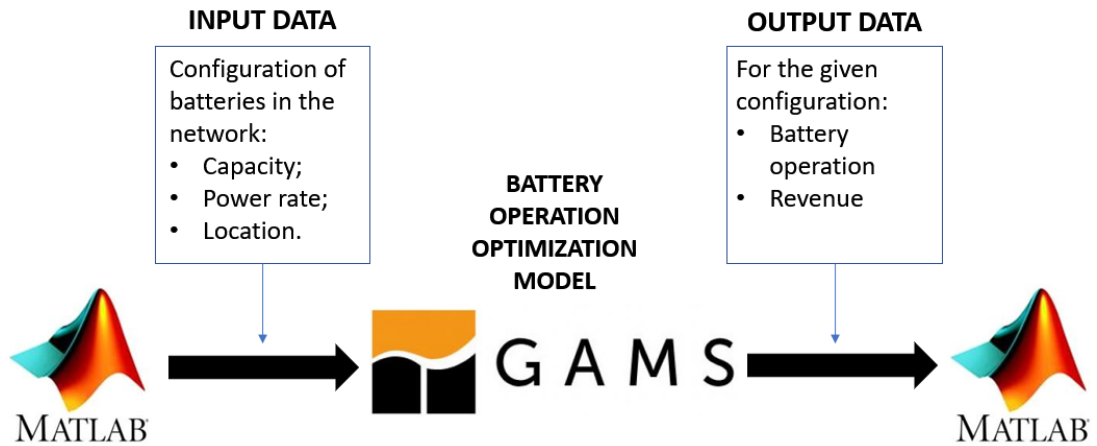


Figure 4-4 - MATLAB/GAMS information exchange

Within the mathematical programming, linear programming can be highlighted. The formulation is described in (Eq. 4.9).

- Linear programming:

$$\begin{aligned}
 & \text{maximize } c^T x \\
 & \text{subject to } Ax \leq b \\
 & \text{and } 0 \leq x \leq \bar{x}
 \end{aligned}
 \tag{Eq. 4.9}$$

4.2.2. GMDH Neural Network

A limitation of modelling a problem by mathematical programming with several restrictions and a vast data set, like the one used in this work, is the high computational effort required. Therefore, in order to reduce the computational effort required by mathematical programming, GMDH neuronal networks were developed.

Figure 4-5 presents the two types of GMDH neuronal networks considered for the proposed model. The first receives as inputs the capacity and charge/discharge rates of the battery and outputs the revenue that that battery configuration can generate in the network at study. The second type of network considered takes as input a particle with the network's battery

configuration and outputs the maximum power flow registered. This way it is possible to penalize battery configurations that result in a violation of the network lines limits.

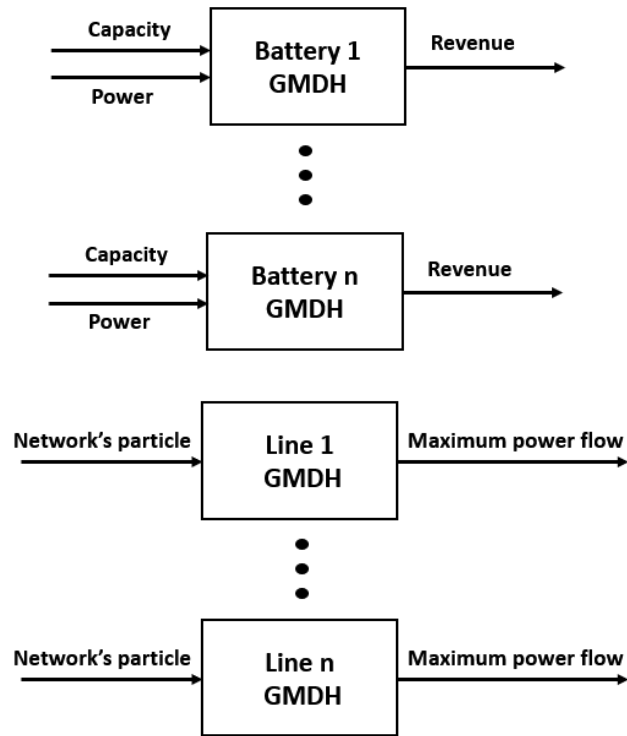


Figure 4-5 - Proposed GMDH architecture

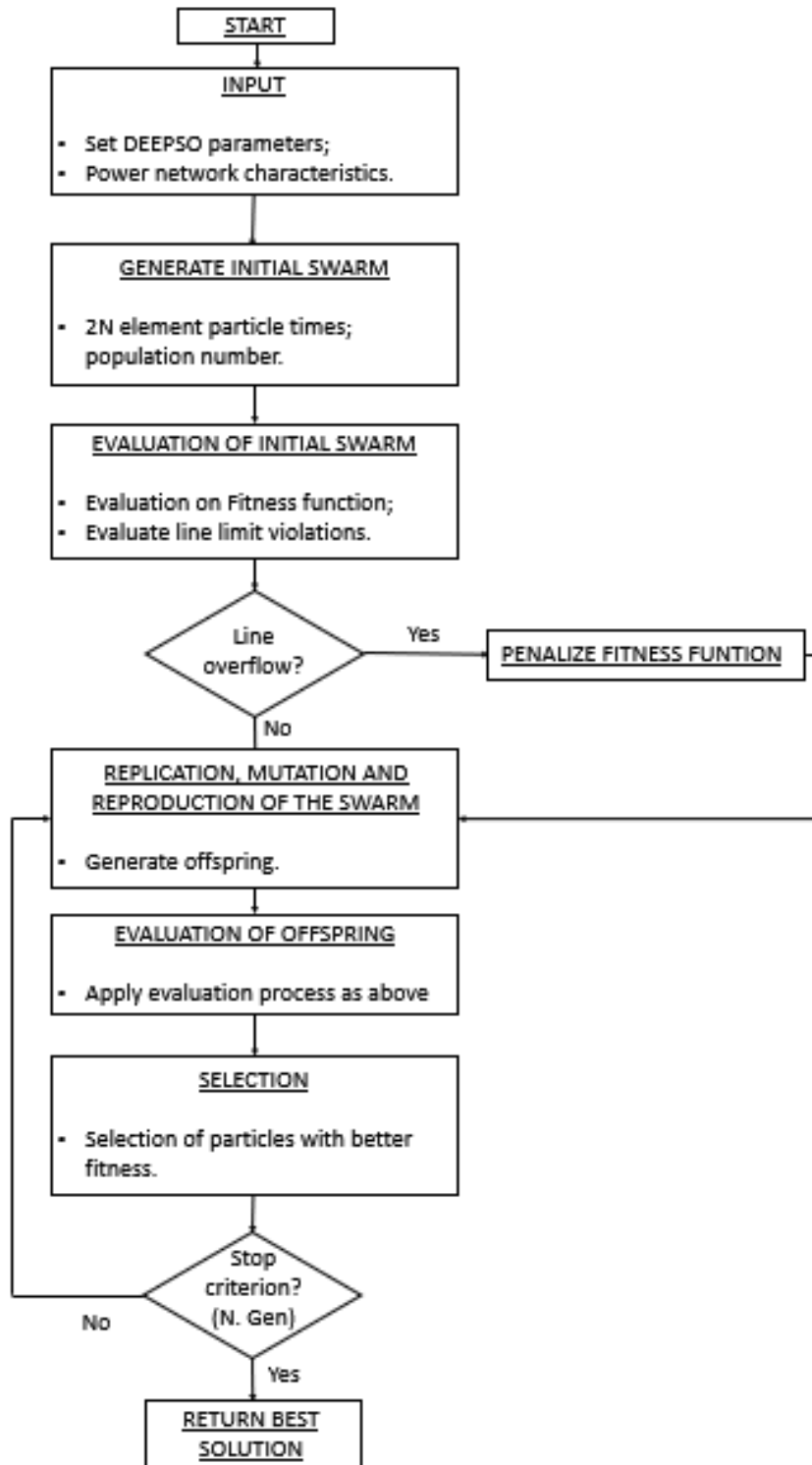


Figure 4-6 - Proposed methodology's flowchart

Chapter 5

Numerical experiments and validation

In this chapter, the proposed methodology will be validated, with a series of experiences in order to prove its adequacy. For this, we will use a modified CIGRE MV distribution benchmark network [50].

5.1. CIGRE MV Distribution Network benchmark

This network follows a European configuration where feeders are three-phase with either meshed or radial structure. The nominal voltage is 20 kV and the frequency is 50 Hz

The chosen topology of the network used for tests follows a radial structure, with switches S1, S2, and S3 open. Both feeders are fed via separate transformers from a 110 kV substation network.

On feeder 1 lines are underground and composed of XPLE cables with round, stranded aluminium conductors and copper tape shields. On feeder 2 lines are aerial and made from aluminium with steel reinforcement.

The parameters of lines and transformers are used to calculate the sensitivity matrix which will be used to calculate the network's power flow. Load data was manipulated according to the daily load curves described in chapter 3 in order to reflect a realistic behaviour for the nominal loads from CIGRE benchmark network resulting in a different daily load curve for every day of the year.

PV generation was included in buses 3 to 6 and buses 8 to 11.

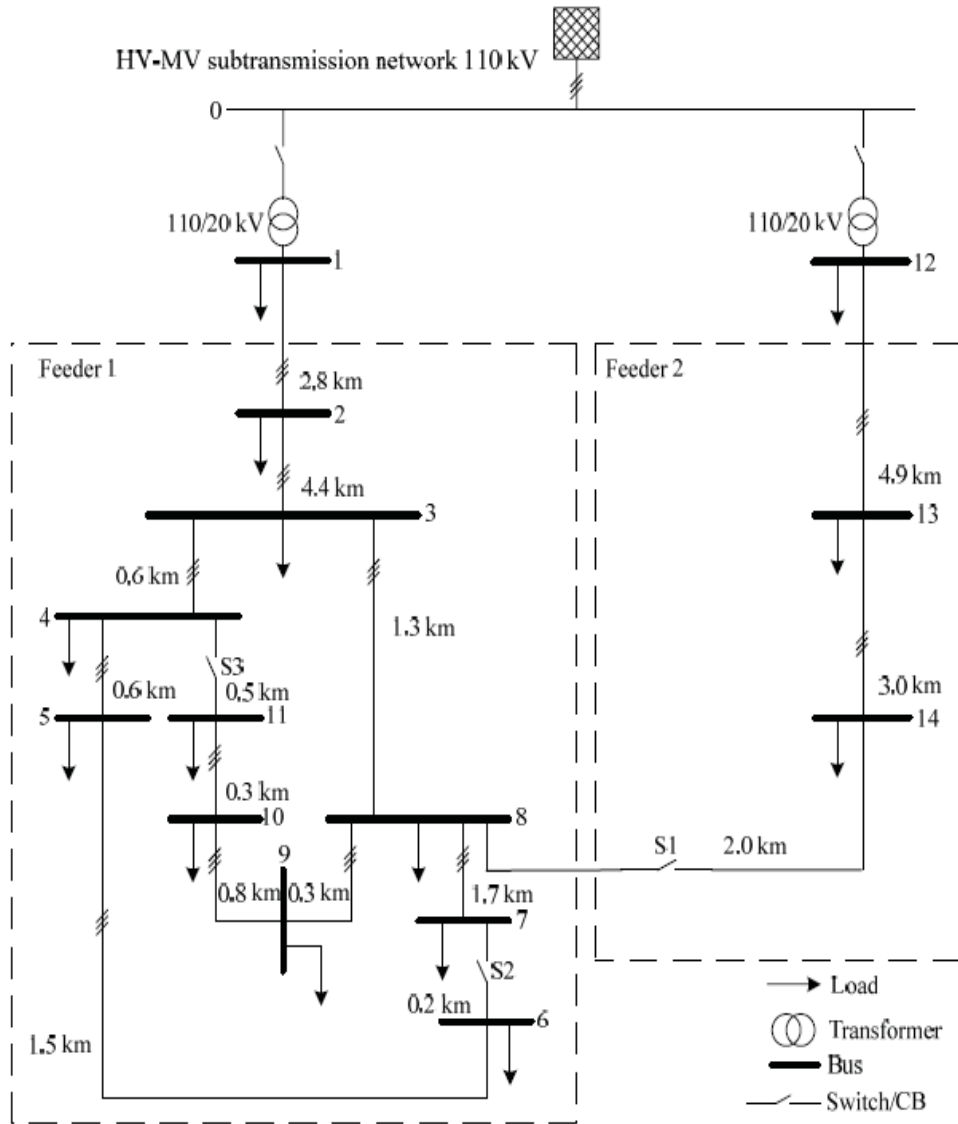


Figure 5-1 - Topology of the CIGRE MV Distribution network benchmark - European configuration

5.2. Stochastic Scenario Creation

As mentioned in Chapter 3, a stochastic scenario of load, generation and prices was created for the following experiments.

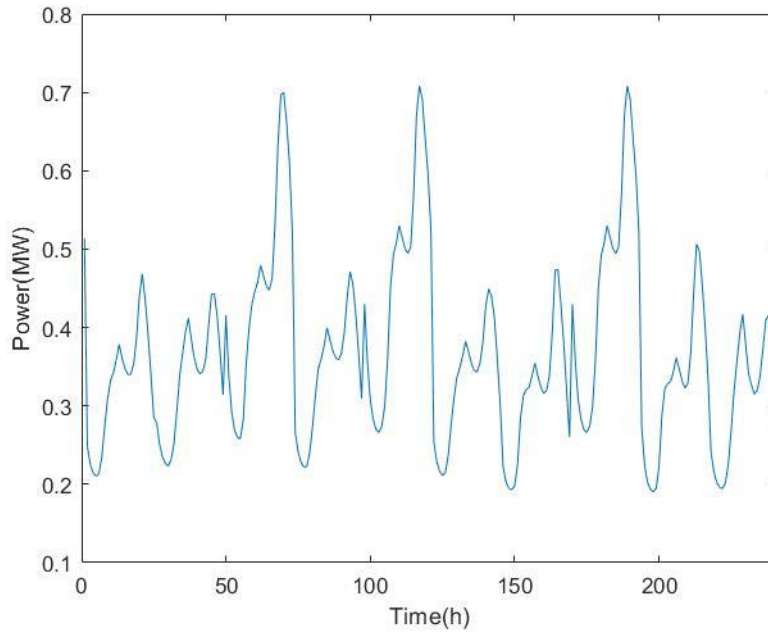


Figure 5-2 - Load in Bus 5 over 10 days

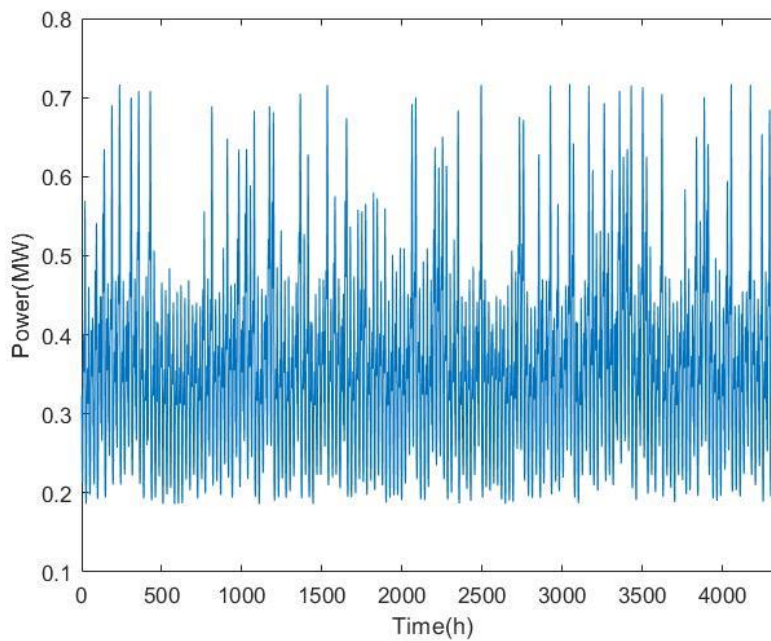


Figure 5-3 - Load in bus 5 over 6 months

As illustrated in Figure 5-2 and Figure 5-3, there is a lot of variability between daily load curves for the same bus, representing days from different seasons as well as differentiation between weekdays and weekend days.

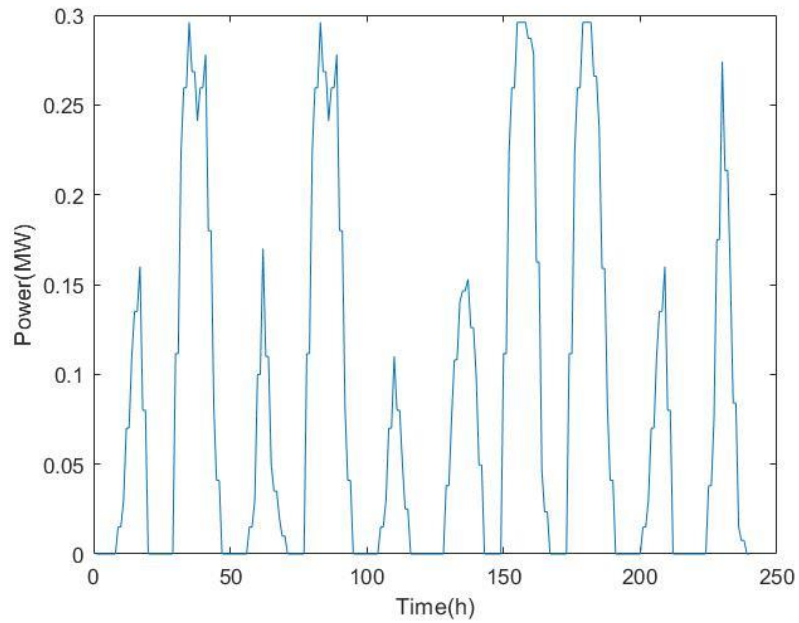


Figure 5-4 - PV Generation in bus 5 over 10 days.

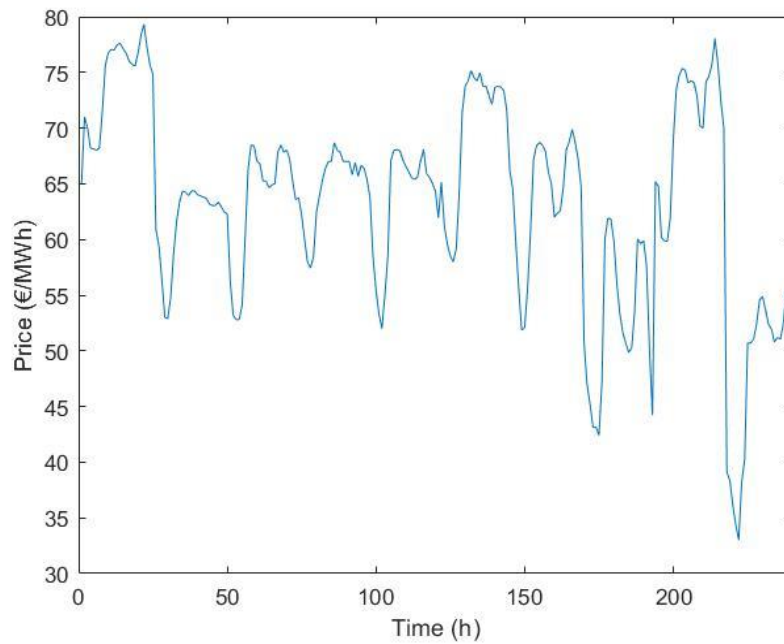


Figure 5-5 - Energy prices over 10 days

5.3. Business model experiments

The methodology described in the previous chapter was tested considering different business models. The objective is to evaluate the feasibility of a business of buying and selling energy through BESS, in distribution networks by entities independent of the distribution network operators. The main objectives will be the identification of a breakeven cost for the business model and then the creation of a conditional decision set. This set is composed by economically viable solutions that will have to be evaluated by the energy provider considering more complex criteria.

For all the business models considered, the following assumptions apply:

- Bess is a price taker, and as such its operation does not affect the market price;
- The characteristics of BESS throughout its life cycle are constant;
- The efficiency of BESS is considered to be 100%;
- It is considered that the BESS can have a depth of discharge of 100%;
- Although the purchase and sale of energy in distribution networks is subject to additional fees, MIBEL's daily market prices were considered;

5.3.1. Bess as a participant in the daily market

Sets:

- b - Set of indices of the network buses;
- t - Set of indices of the hourly time periods

Parameters:

- Ep_t - Market clearing price for time t ;
- $\underline{SoC}, \overline{SoC}$ - Minimum and maximum state of charge of the BESS, respectively
- \overline{Pr}_b - Maximum charge/discharge power of the BESS

Variables:

- $Bg_{b,t}$ - Discharging phase of the BESS;
- $Bl_{b,t}$ - Charging phase of the BESS;
- $SoC_{b,t}$ - State of charge of the BESS;

The main objective considered is the maximization of the battery's revenue considering energy price values, (Eq. 5.1). The state of charge, SoC , in any t , is calculated from the previous SoC and the energy balance of the operation of the battery, (Eq. 5.2). The SoC is limited by the maximum energy capacity of the battery and by a lower limit defined by the user, (Eq. 5.3). Bl and Bg are limited by zero and by the maximum power rating of the battery, (Eq. 5.3) and (Eq. 5.5).

$$\max \sum_b^{bus} \sum_t^{time} (Ep_t (Bg_{b,t} - Bl_{b,t})) \quad (\text{Eq. 5.1})$$

$$\forall_b \forall_t SoC_{b,t} = SoC_{b,t-1} + Bl_{b,t} - Bg_{b,t} \quad (\text{Eq. 5.2})$$

$$\forall_b \forall_t \underline{SoC} \leq SoC_{b,t} \leq \overline{SoC} \quad (\text{Eq. 5.3})$$

$$\forall_b \forall_t 0 \leq Bl_{b,t}, Bg_{b,t} \quad (\text{Eq. 5.4})$$

$$\forall_b \forall_t Bl_{b,t}, Bg_{b,t} \leq \overline{Pr}_b \quad (\text{Eq. 5.5})$$

$$\forall_b SoC_{b,1} = \overline{SoC} \cdot 0.5 \quad (\text{Eq. 5.6})$$

For the testing of this business model, 3 price scenarios of battery investment costs were used. Further increments in price were not analyzed in this work as they were not deemed economically viable.

Table 5.1 - Capital investment scenario definition

Scenario	Very Optimistic	Optimistic	Breakeven
Power Costs (€/kW)	82.5	90	97.5
Energy Costs (€/kWh)	55	60	65
Maintenance Costs (€/kWh)	0.100	0.100	0.100

All buses in the network were considered as possible locations for a battery, except bus 15, which is used as the slack bus. The maximum battery capacity was limited to 1 MWh.

5.3.1.1. Battery Operation

In this section the operation of a 1MWh and 0.4 MW battery optimized by LP was analyzed. As noted in Figure 5-6, the battery waits for the periods when the energy is cheaper to charge and stores the energy until a point of greater economic value.

40 Numerical experiments and validation

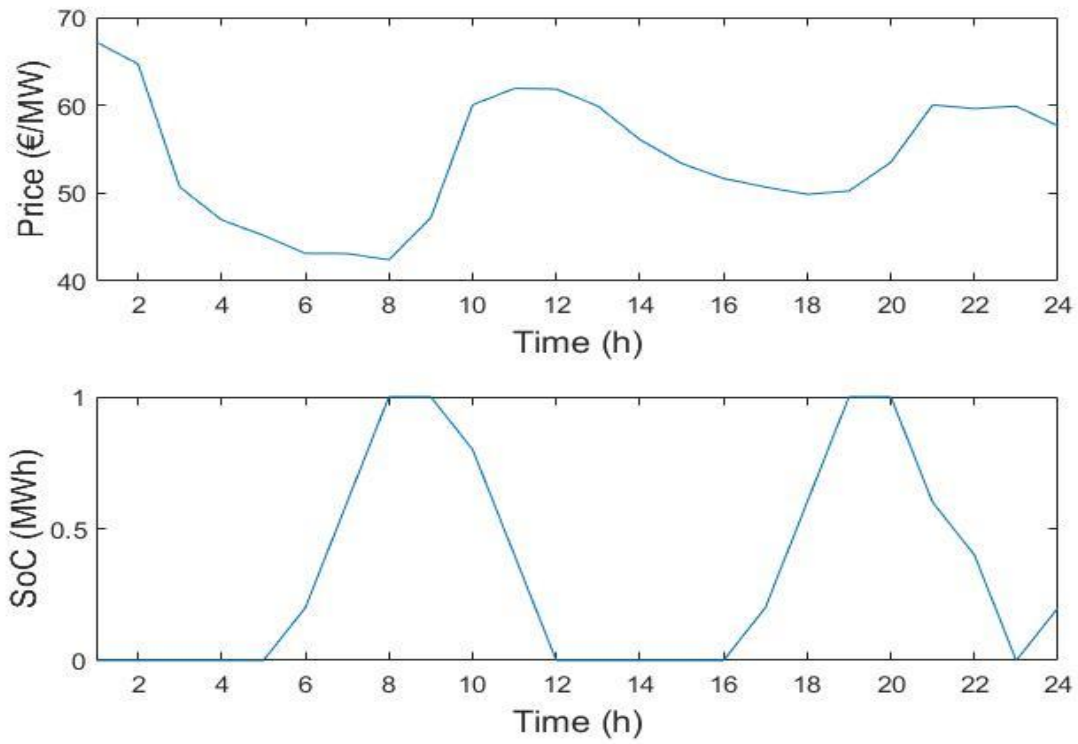


Figure 5-6 - Battery operation (down) relative to energy price (up) over 1 day

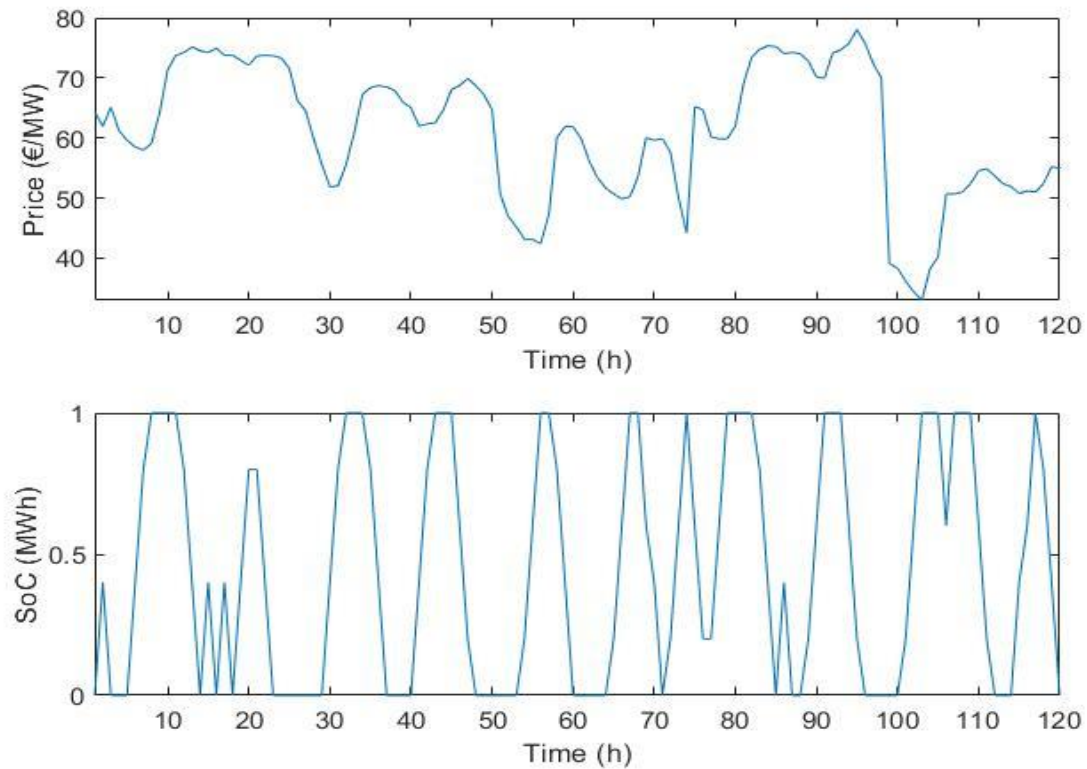


Figure 5-7 - Battery operation (down) relative to energy price (up) over 5 days

With an analysis with a longer time horizon, it is proved that the battery has very different behaviors depending on the market curve for the day in question (Figure 5-7).

5.3.1.2. Results

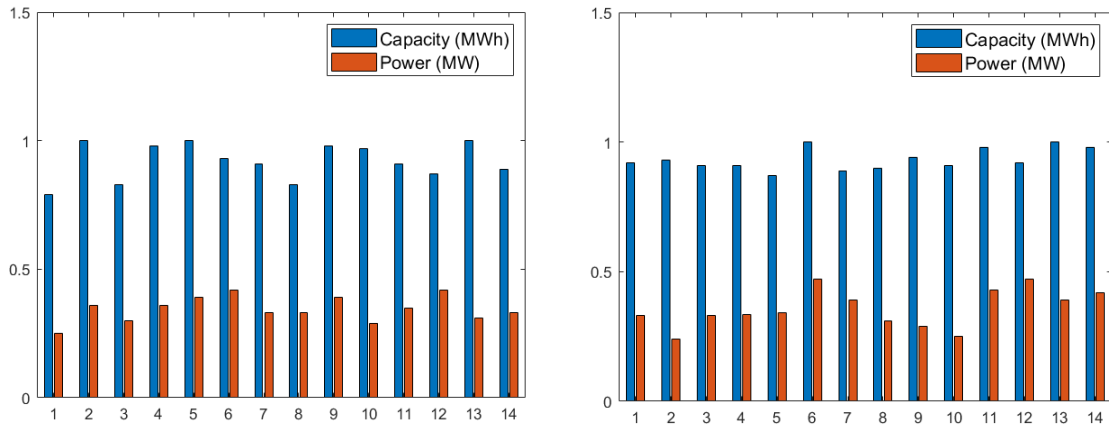


Figure 5-8 - Examples of solutions for the very optimistic scenario that compound the conditional decision set

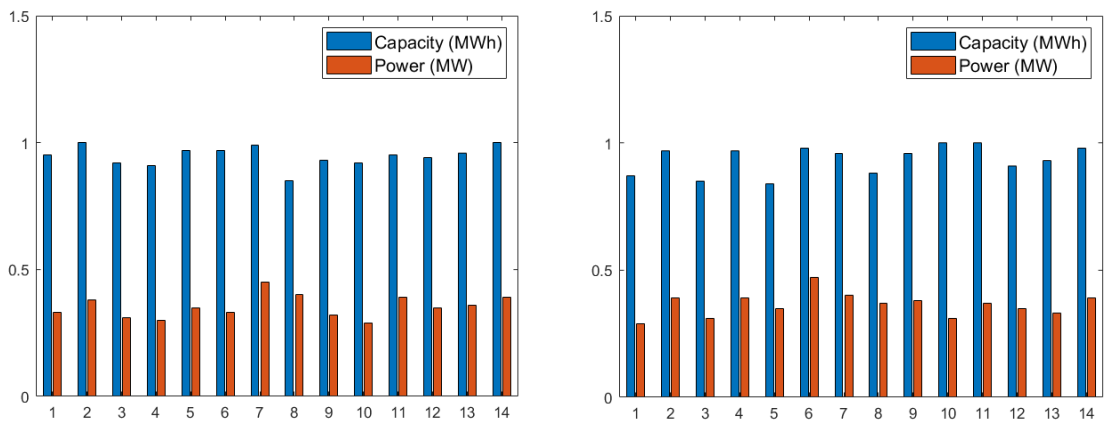


Figure 5-9 - Examples of solutions for the optimistic scenario that compound the conditional decision set

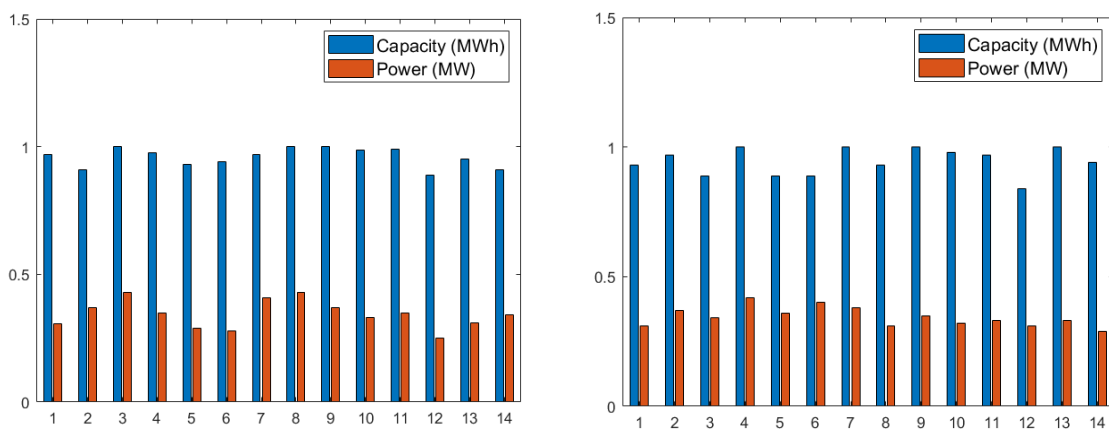


Figure 5-10 - Examples of solutions for the break-even scenario that compound the conditional decision set

In Figure 5-8, Figure 5-9 and Figure 5-10 are shown examples of final solutions obtained for the 3 scenarios considered. DEEPSO used a 40 particles swarm for 100 iterations. It is noticeable that the differences in the solutions found are quite small between the all the scenarios evaluated, this fact supports the idea about the necessity of a conditional decision set as these small differences may not pose much difference with the criteria defined for this business model but a better distinction may arise if more applications of the BESS are added to the main business model. This occurs because the addition of other applications such as loss reduction, reliability, voltage support and ancillary services must be tested under an AC power flow model, which means more detailed and complex network model.

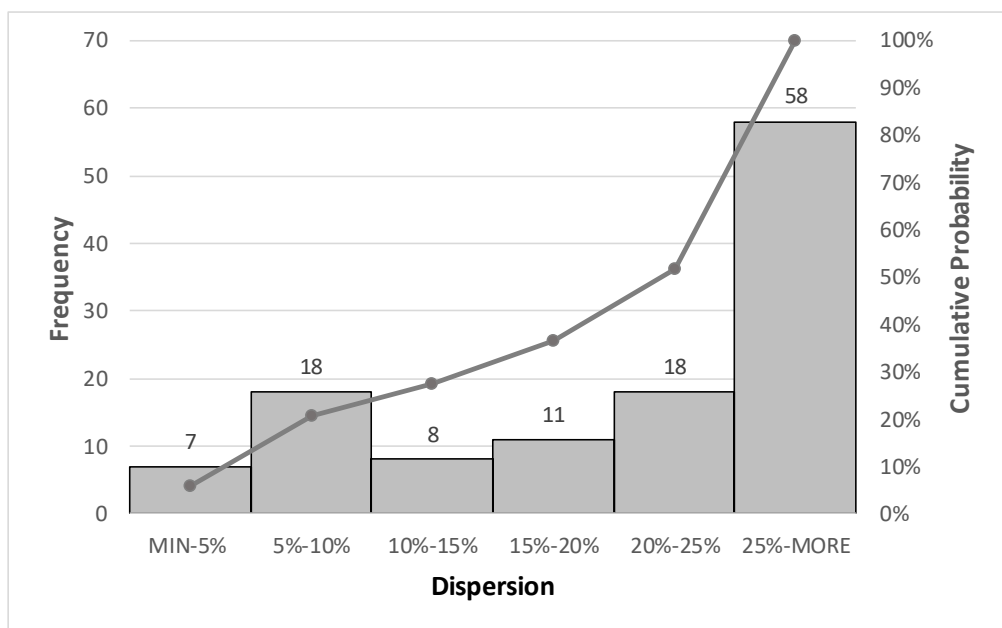


Figure 5-11 - 5% step of dispersion histogram of the results of solutions for the very optimistic scenario.

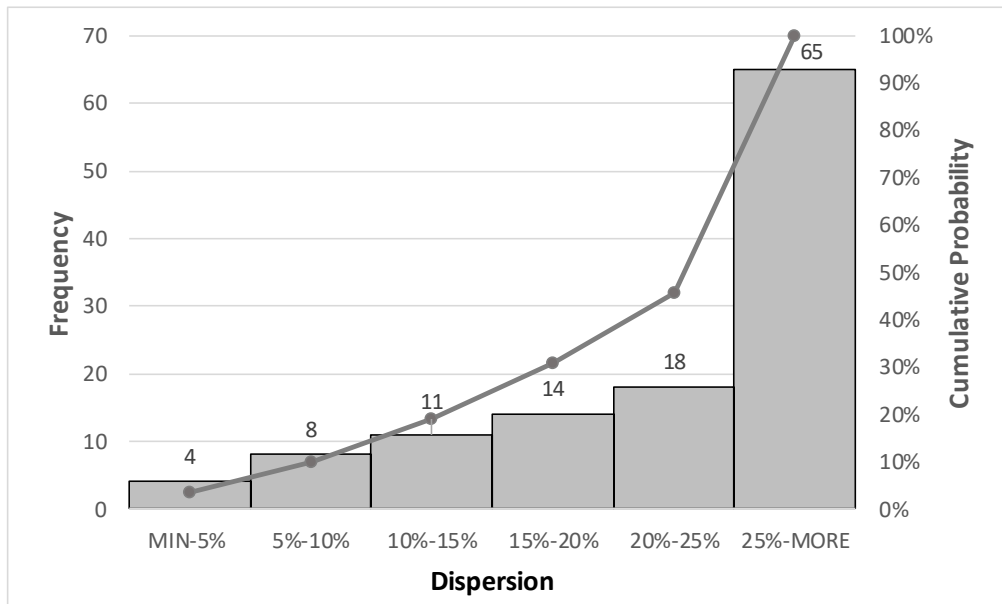


Figure 5-12 - 5% step of dispersion histogram of the results of solutions for the optimistic scenario.

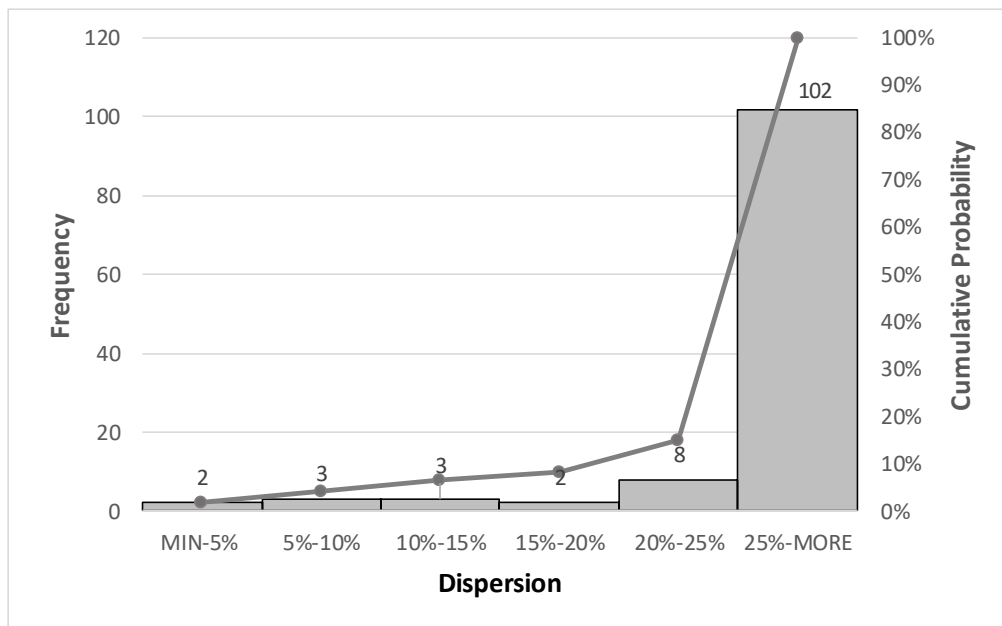


Figure 5-13 - 5% step of dispersion histogram of the results of solutions for the break-even scenario.

For supporting the investment planning decision-making from an energy provider perspective, a good-quality conditional decision set of optimal solutions economically viable for the business model of buying and selling energy is built based on the consideration that the solutions selected must be in the first 5%-step of dispersion in order to guarantee that no only one solution, frequently called best solution, is reported as the most interesting solution that

solves the problem. Under this assumption, other economically viable solutions located close to the best solution are identified for evaluating them and analyze which of them could be properly selected to enhance the economic benefits as results of establishing synergies between different applications of BESS. The results of the 5%-step of dispersion histogram for the scenarios cost analyzed are shown in Figure 5-11, Figure 5-12 and Figure 5-13. As noted, in the first 5%-step a representative quantity of solutions are found. Nonetheless, the quantity of solution to compound the conditional decision set decreases when the scenario cost is closer to the breakeven, which supports the idea that only a few solutions in this scenario allows the main business model becomes profitable for the energy provider.

5.3.2. Bess coupled with PV as a participant in the daily market

For this model the energy provider is the owner of PV generation within the distribution network and wants to include BESS technology in his business. An extra consideration must be emphasized in this model, since the price attributed to PV generation is normally set at auction. However, with this format, no economic benefit could exist through time-shifting with a BESS. To do this, it is necessary to consider a scenario with price variations that allows the battery the possibility of transferring energy between periods leading to greater economic gain. As such, in this analysis, the prices of the daily energy market of MIBEL were used.

Sets

- b - Set of indices of the network buses;
- t - Set of indices of the hourly time periods

Parameters

- Ep_t - Market clearing price for time t ;
- $\underline{SoC}, \overline{SoC}$ - Minimum and maximum state of charge of the BESS, respectively;
- \overline{Pr}_b - Maximum charge/discharge power of the BESS;
- $Ger_{b,t}$ - PV generation;

Variables

- $Bg_{b,t}$ - Discharging phase of the BESS;
- $Bl_{b,t}$ - Charging phase of the BESS;
- $SoC_{b,t}$ - State of charge of the BESS;

The difference in this model lies in (Eq. 5.6) where parameter Ger is considered. This way energy from PV generation is either stored in the battery or sold in the market.

$$\max \sum_b^{bus} \sum_t^{time} (Ep_t (Bg_{b,t} + Ger_{b,t} - Bl_{b,t} +)) \quad (\text{Eq. 5.7})$$

$$\forall_b \forall_t SoC_{b,t} = SoC_{b,t-1} + Bl_{b,t} - Bg_{b,t} \quad (\text{Eq. 5.8})$$

$$\forall_b \forall_t \underline{SoC} \leq SoC_{b,t} \leq \overline{SoC} \quad (\text{Eq. 5.9})$$

$$\forall_b \forall_t 0 \leq Bl_{b,t}, Bg_{b,t} \quad (\text{Eq. 5.10})$$

$$\forall_b \forall_t Bl_{b,t}, Bg_{b,t} \leq \overline{Pr}_b \quad (\text{Eq. 5.11})$$

$$\forall_b SoC_{b,1} = \overline{SoC} \cdot 0.5 \quad (\text{Eq. 5.12})$$

The investment scenarios were those present in Table 5.1. In this case, only buses that had PV generation were considered as possible buses for placing batteries. This is as if the PV generation and the BESS were placed in different buses, the energy provider would have to pay network usages fees, and such fees are not considered in this work. The maximum battery capacity was limited to 1 MWh.

5.3.2.1. Battery Operation

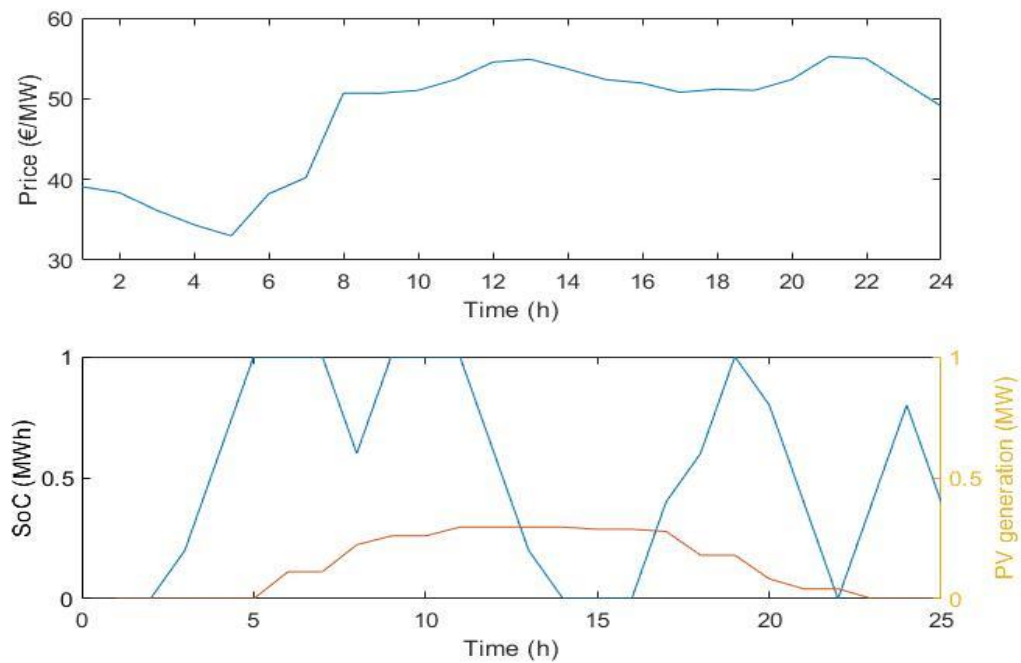


Figure 5-14 - - Battery operation (down) relative to energy price (up) over 1 day

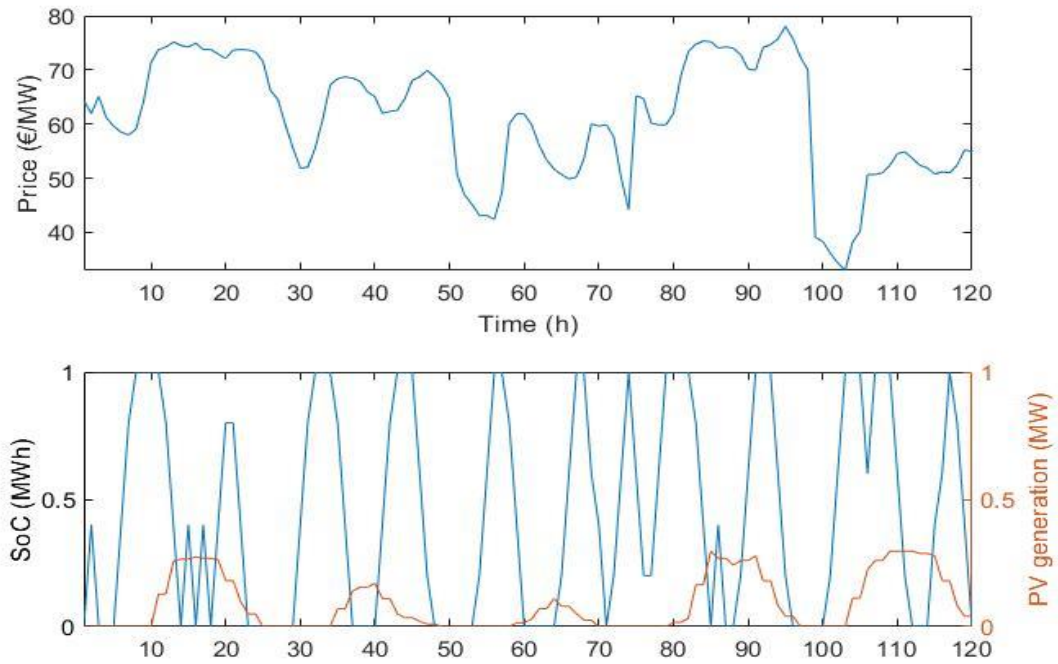


Figure 5-15 - - Battery operation (down) relative to energy price (up) over 5 days

As can be noted from Figure 5-14, the battery waits for the periods when the energy has less value to charge and stores the energy until a point of greater economic value, just like in the first model analyzed. Another conclusion that can be made from Figure 5-15 is that the battery's operation is similar to the operation for the previous model. This suggests for a business model such as that established in this chapter, the addition of a BESS to the PV does not lead to a greater economic gain compared to operating them separately. This can be attributed mainly to two factors: Firstly, PV production usually occurs at times when energy is more expensive, so it is beneficial to sell energy immediately to the grid. Second, the BESS will be able to maximize its profit if it can buy the maximum amount of energy in periods of lower prices, other than holding energy from PV to sell to sell in subsequent periods with a lesser margin.

5.3.2.2. Results

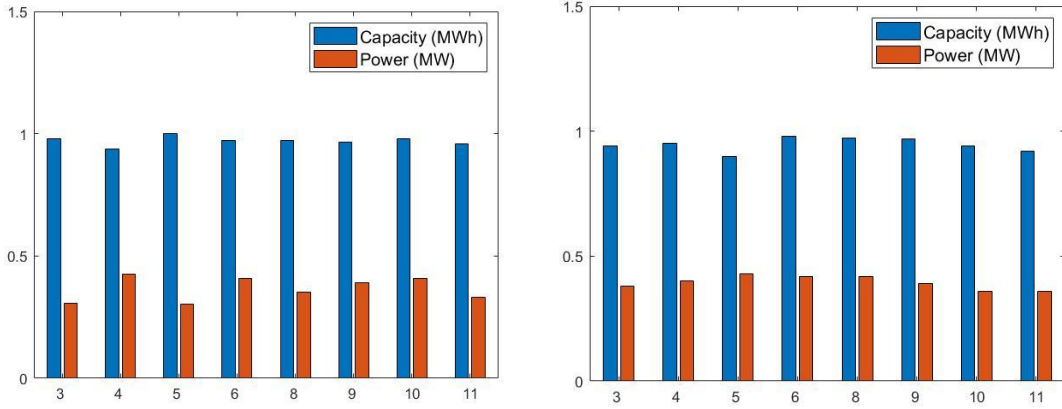


Figure 5-18 - Examples of solutions for the very optimistic scenario that compound the conditional decision set

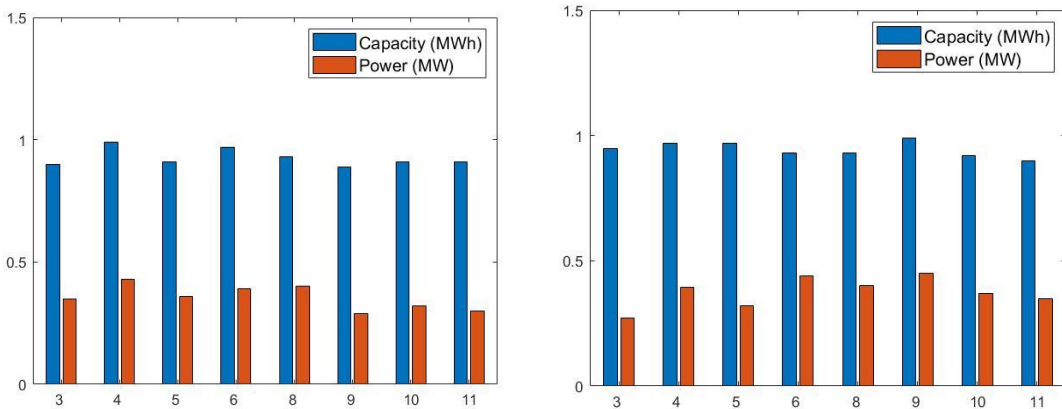


Figure 5-17 - Examples of solutions for the optimistic scenario that compound the conditional decision set

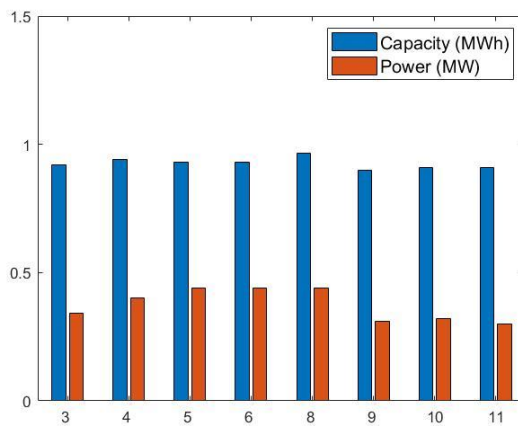


Figure 5-16 - Solution for the break-even scenario that compound the conditional decision set

In Figure 5-18, Figure 5-17 and Figure 5-16 are shown examples of final solutions obtained for the 3 scenarios considered. DEEPSO used a 40 particles swarm for 100 iterations. It is, again, noticeable that the differences in the solutions found are quite small between the all the scenarios evaluated. A similar result to the previous model was expect because, just like was observed in section 5.3.2.1 the PV doesn't affect the battery operation.

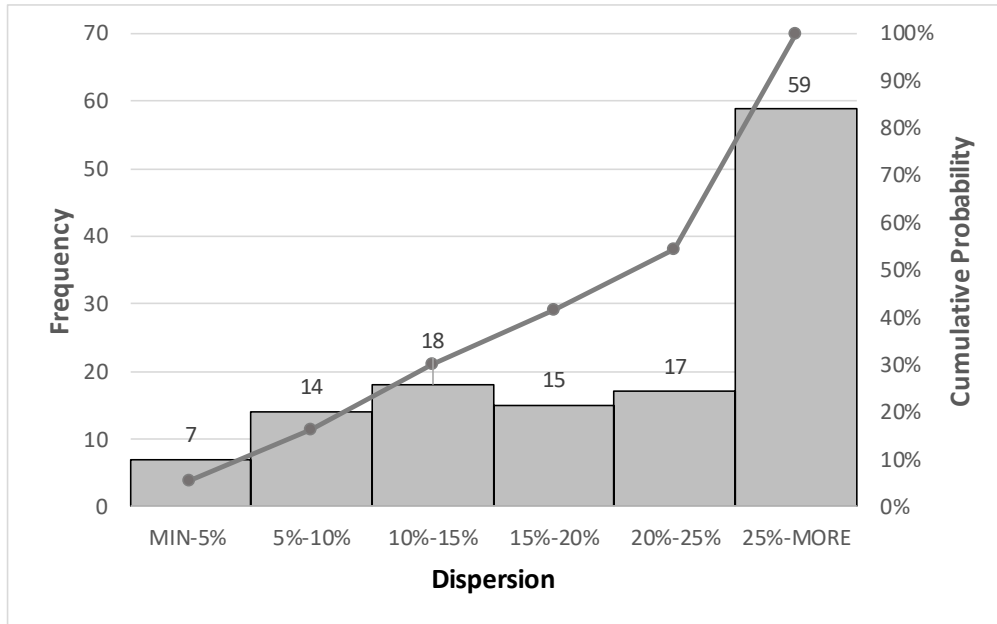


Figure 5-19 - 5% step of dispersion histogram of the results of solution for the very optimistic scenario.

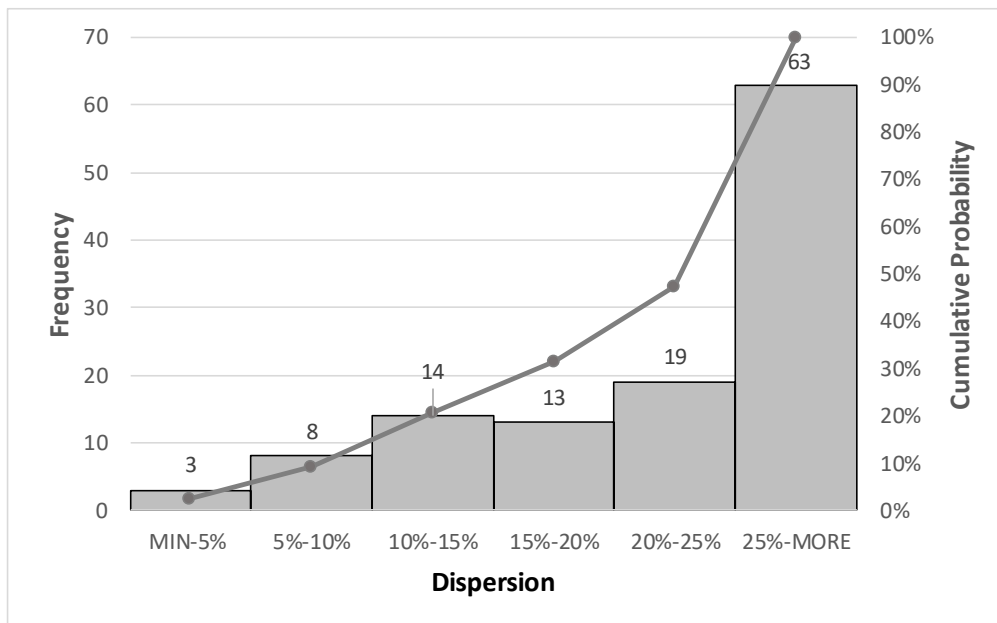


Figure 5-20 - 5% step of dispersion histogram of the results of solution for the optimistic scenario.

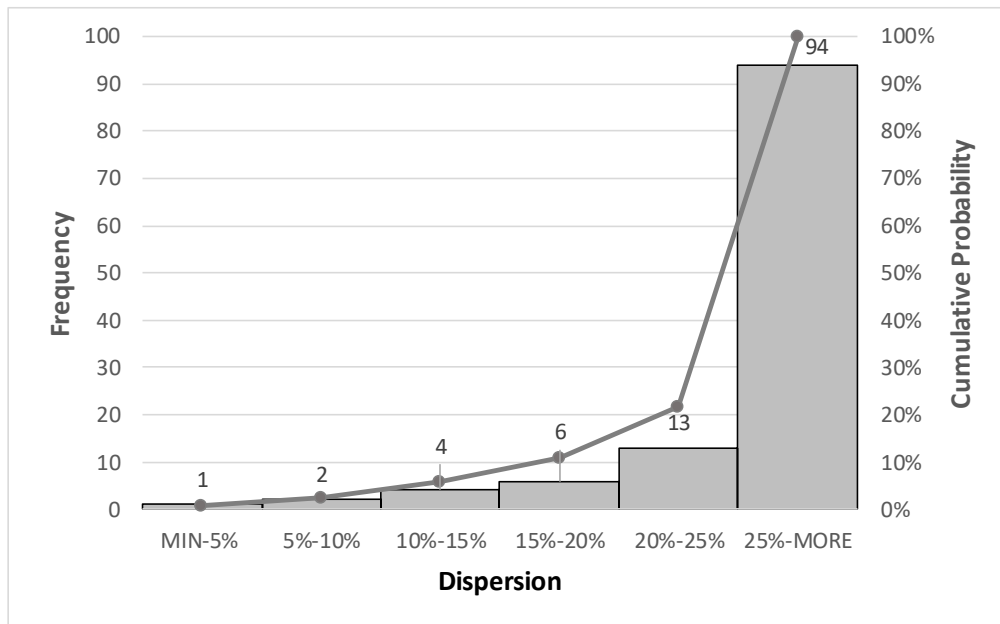


Figure 5-21 - 5% step of dispersion histogram of the results of solutions for the break-even scenario.

5.4. Methods Validation

5.4.1. GMDH vs mathematical programming

In this chapter a comparison of the use of only mathematical programming versus its combination with the use of the GMDH will be made for the scenario exposed in 5.2.1. However, due to time constraints for carrying out this work and considering the fact that a simulation using only mathematical programming has a high execution time, the stochastic scenario under study will only have a total of 120 days as opposed to the 365 used for the previous sections.

For the period described, the results for the 3 investment scenarios considered to be viable are analyzed, and the performance of the algorithm is compared in a scenario where it uses only LP, and the scenario in which it uses LP and GMDH networks. For each test the same random number generator was used, so that any differences observed are a reflection of the evaluation method used. As a result of this, until the iteration in which the GMDH is trained is reached, the cost evolution will have the same behavior. In addition, since the computational effort of an iteration using GMDH is very low, twice as many iterations were performed as for the case that only uses LP.

50 Numerical experiments and validation

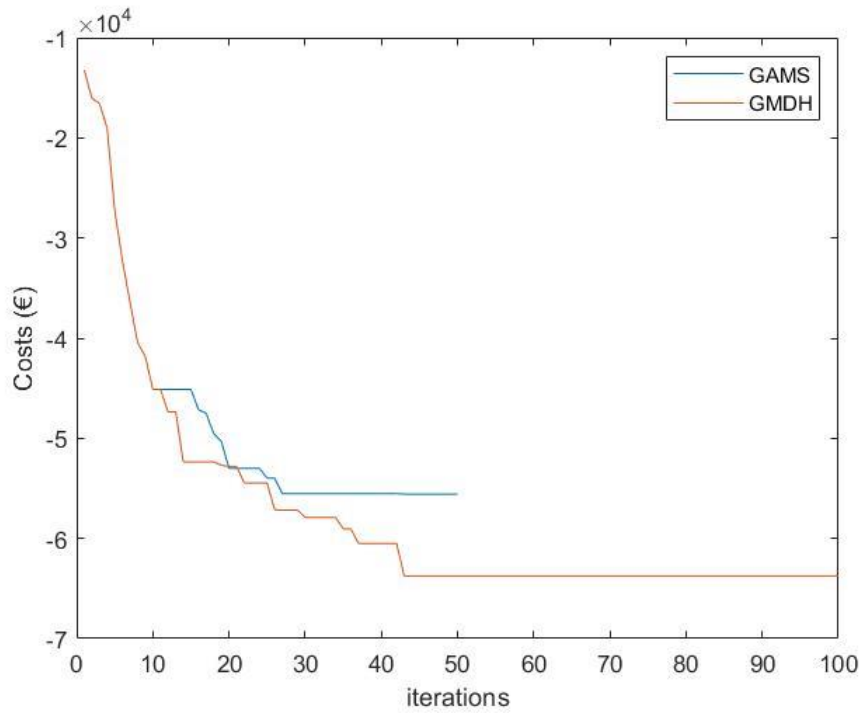


Figure 5-22 - Comparison of the evolution of the cost best particle found by DEEPSO using just LP (GAMS) or using LP and GMDH (GMDH) for the very optimistic scenario, simulation 1.

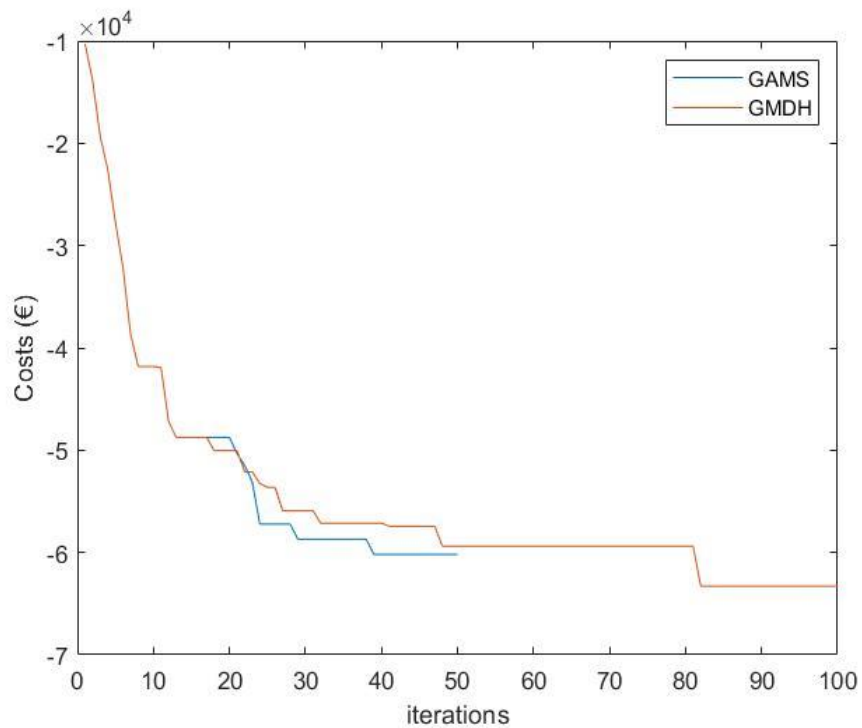


Figure 5-23 - Comparison of the evolution of the cost best particle found by DEEPSO using just LP (GAMS) or using LP and GMDH (GMDH) for the very optimistic scenario, simulation 2.

Figure 5-22 and Figure 5-23, represent simulations with the same parameters, except for the random number generator. As can be noted, from the 10th iteration on, (the iteration in which GMDH is trained) the cost curves diverge. This is due to small differences in the evaluation of the solutions, converging to a better solution in slightly different ways. It should be noted that the error in calculating the battery operation by GMDH was only of 1.24% for the scenario in Figure 5-22 and 1.3% for the scenario in Figure 5-23.

With this in mind, the version with GMDH alone finds a superior solution, since the cost of the solution is still better since the difference for the solution found by the LP solution is larger than the network evaluation error. However, this may not happen, and the evaluation by LP alone find the better solution, as shown in the figure below. Until interaction 50, the LP version seemed to have found a better solution. Despite this, due to the possibility of performing a large number of iterations with GMDH, this option ends up finding a better solution. The same conclusions can be extended to the remaining investment scenarios for which the results presented in imagens.

In relation to computational time, a single iteration using LP lasted an average of 784 seconds, that time can be reduced to around 1 second using GMDH networks. This enormous decrease in computational time is even larger when the 365-day scenario is considered as the same time would be obtained from GMDH networks, 1 second, while LP time vastly increases to 3769 seconds.

52 Numerical experiments and validation

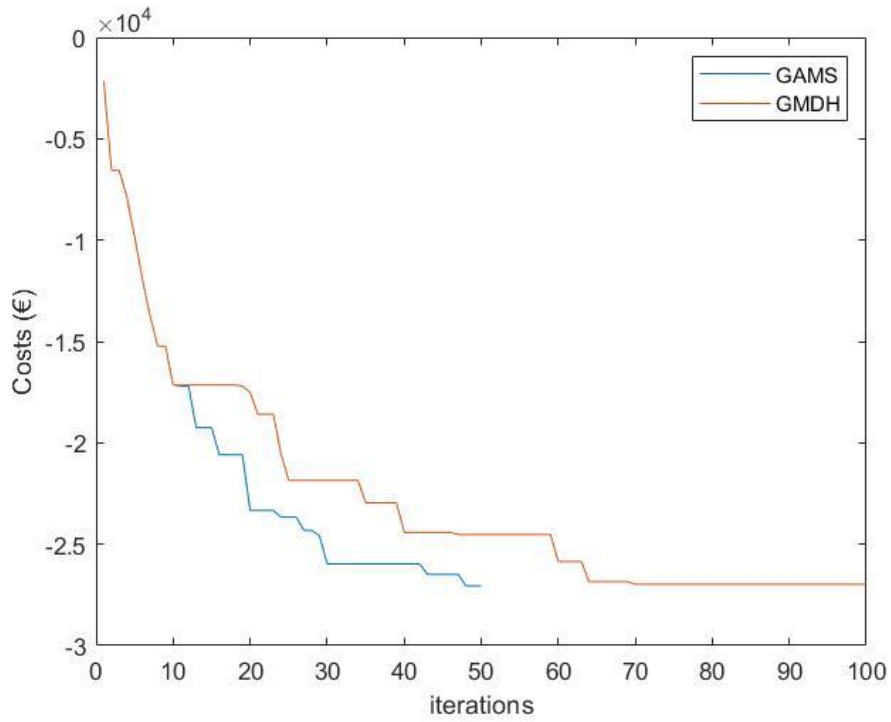


Figure 5-24 - Comparison of the evolution of the cost best particle found by DEEPSO using just LP (GAMS) or using LP and GMDH (GMDH) for the optimistic scenario

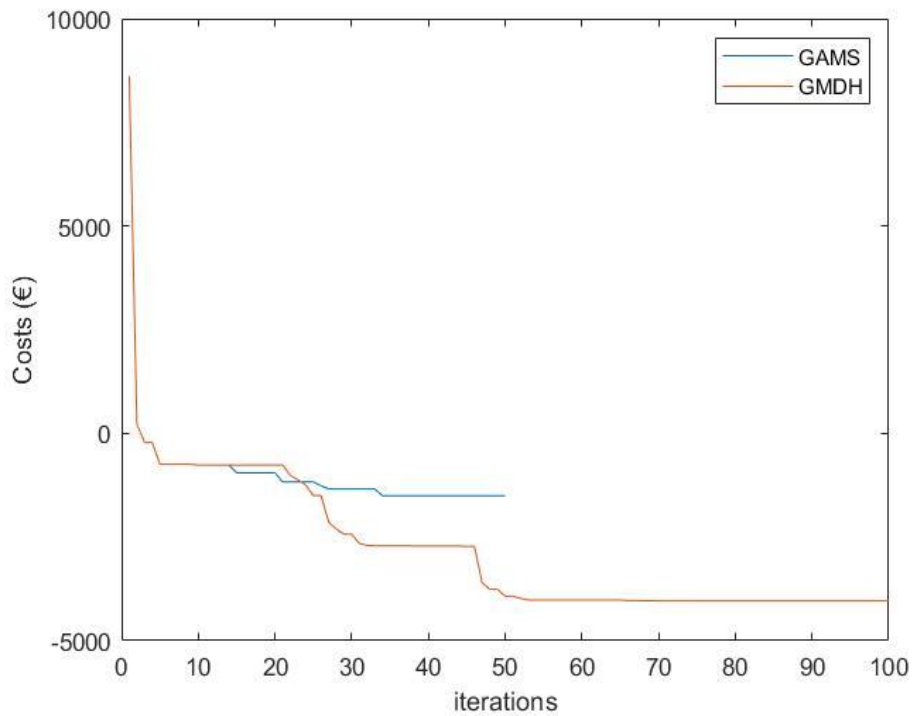


Figure 5-25 - Comparison of the evolution of the cost best particle found by DEEPSO using just LP (GAMS) or using LP and GMDH (GMDH) for the break-even scenario

Chapter 6

Conclusions and Future Work

6.1. Conclusions

A model for supporting the investment planning decision-making from a perspective of an independent energy provider that wants to obtain a conditional decision set that can be evaluated for multiple decision criteria such as loss reduction, reliability, voltage support, ancillary services, etc. was proposed, in order to raise the profitability of integrating BESS in the distribution networks. For this, it was modelled the main economical compromises between (i) the investment costs and BESS application as a business model of purchasing and sale energy at a day ahead market price; and (ii) the investment costs and options for sizing, location, and BESS operation as an optimization model based on the DEEPSO-GMDH approach.

Although with a scope limited to the system tested, interesting conclusions could be drawn. From the perspective of an independent energy provider, the integration of BESS is non-profitable at the current value cost of the batteries when a business model based on the purchase and sales of energy in the day ahead energy market was evaluated. Then, it becomes mandatory to establish the breakeven cost of investment planning for integrating BESS guarantee the start point where the business model becomes profitable. To identify a conditional decision set of optimal solutions economically viable for the business model of buying and selling energy makes possible to reduce the combinatorial behavior of modelling the investment plan required for integrating BESS in distribution networks where profitable businesses are searched for an independent energy provider while the sizing, location, and operation of BESS are optimized. From this conditional decision set of optimal solutions, other business models can be evaluated to raise the economic benefits an energy provider can receive if synergies between business model for BESS are established. Nevertheless, it is important to highlight that each optimal solution must be evaluated on an AC power flow model for

representing a realistic network scenario where characteristics such as voltage profile, losses, and AC power flow are considered because these characteristics can mark differences between optimal solutions evaluated when one or several applications of the BESS want be added to the main business model.

6.2. Future work

The work developed over this thesis contributes to the study of the sizing, location and optimization of the operation of batteries. However, the methodology can be improved, and some suggestions will be presented to further develop this work:

- GMDH was able to dramatically reduce computational time by iteration, however, it remains high since some iterations by LP are necessary for neural networks to be trained. Therefore, options to reduce this computational time should be evaluated, such as optimizing the GAMS model;
- The development of an AC model that allows testing other battery applications in order to obtain a better distinction from the conditional decision set obtained;
- Only one business model for buying and selling energy in the daily market was approached, however, other models could be promising, such as the secondary reserve market and the tertiary reserve market;
- The introduction of a degradation model of the batteries based on the number of cycles and their depth of charge instead of relying on its life expectancy in years might condition the operation of the battery and result in a more realistic result.

References

- [1] C. K. Das, O. Bass, G. Kothapalli, T. S. Mahmoud, and D. Habibi, 'Overview of energy storage systems in distribution networks: Placement, sizing, operation, and power quality', *Renew. Sustain. Energy Rev.*, vol. 91, no. March, pp. 1205-1230, Aug. 2018. C. J. Joubert, N. Chokani, and R. S. Abhari, "Impact of Large Scale Battery Energy Storage on the 2030 Central European Transmission Grid," in 2018 15th International Conference on the European Energy Market (EEM), 2018, vol. 2018-June, pp. 1-5.
- [2] F. Teng, M. Aunedi, R. Moreira, G. Strbac, P. Papadopoulos, and A. Laguna, 'Business case for distributed energy storage', *CIREC - Open Access Proc. J.*, vol. 2017, no. 1, pp. 1605-1608, Oct. 2017.
- [3] F. Nadeem, S. M. S. Hussain, P. K. Tiwari, A. K. Goswami, and T. S. Ustun, "Comparative review of energy storage systems, their roles, and impacts on future power systems," *IEEE Access*, vol. 7, no. c, pp. 4555-4585, 2019.
- [4] H. Saboori, R. Hemmati, S. M. S. Ghiasi, and S. Dehghan, 'Energy storage planning in electric power distribution networks - A state-of-the-art review', *Renew. Sustain. Energy Rev.*, vol. 79, no. May, pp. 1108-1121, Nov. 2017.
- [5] P. Lombardi and F. Schwabe, 'Sharing economy as a new business model for energy storage systems', *Appl. Energy*, vol. 188, pp. 485-496, Feb. 2017.
- [6] R. Dufo-López and J. L. Bernal-Agustín, 'Techno-economic analysis of grid-connected battery storage', *Energy Convers. Manag.*, vol. 91, pp. 394-404, Feb. 2015.
- [7] EASE/EERA, "European energy storage technology development roadmap - 2017 update," p. 128, 2017.
- [8] H. Chen, T. N. Cong, W. Yang, C. Tan, Y. Li, and Y. Ding, "Progress in electrical energy storage system: A critical review," *Prog. Nat. Sci.*, vol. 19, no. 3, pp. 291-312, 2009.
- [9] <https://depts.washington.edu/matseed/batteries/MSE/index.html>. [Accessed: 04-Aug-2019].
- [10] A. C. Hua and B. Z. Syue, "Charge and discharge characteristics of lead-acid battery and LiFePO4 battery," *The 2010 International Power Electronics Conference - ECCE ASIA -*, Sapporo, 2010, pp. 1478-1483.
- [11] H. Keshan, J. Thornburg, and T. S. Ustun, "Comparison of lead-acid and lithium ion batteries for stationary storage in off-grid energy systems," in *4th IET Clean Energy and Technology Conference (CEAT 2016)*, 2016, pp. 30 (7 .)-30 (7 .).
- [12] A. A. Akhil et al., "DOE/EPRI Electricity Storage Handbook in Collaboration with NRECA," no. September, 2016
- [13] J. Cho, S. Jeong, and Y. Kim, "Commercial and research battery technologies for electrical energy storage applications", *Prog. Energy Combust. Sci.*, vol. 48, pp 84-101, 2015
- [14] M. S. Guney and Y. Tepe, "Classification and assessment of energy storage systems," *Renew. Sustain. Energy Rev.*, vol. 75, no. October 2016, pp. 1187-1197, 2017
- [15] "EPRI-DOE Handbook of Energy Storage for Transmission & Distribution Applications," 2003.
- [16] B. DIRECTIVE AND 2013/56/EU, "Batteries Regulations Amendment," *Dep. Business, Inoov. Ski.*, vol. 32, no.5. pp. 349-366, 2014.

- [17] V. A. Boicea, "Energy storage technologies: The past and the present," *Proc. IEEE*, vol. 102, no. 11, pp. 1777-1794, 2014.
- [18] S. Hameer and J. L. van Niekerk, "A review of large-scale electrical energy storage," *Int. J. Energy Res.*, vol. 39, no. 9, pp. 1179-1195, Jul. 2015.
- [19] E. Technology, "Review of electrical energy storage technologies and systems and of their potential for the UK," 2004.
- [20] H.-F. Shen, X.-J. Zhu, M. Shao, and H. Cao, "Neural Network Predictive Control for Vanadium Redox Flow Battery," *J. Appl. Math.*, vol. 2013, pp. 1-7, 2013.
- [21] S. Vazquez, S. M. Lukic, E. Galvan, L. G. Franquelo, and J. M. Carrasco, "Energy storage systems for transport and grid applications," *IEEE Trans. Ind. Electron.*, vol. 57, no. 12, pp. 3881-3895, 2010.
- [22] H. IBRAHIM, A. ILINCA, and J. PERRON, "Energy storage systems—Characteristics and comparisons," *Renew. Sustain. Energy Rev.*, vol. 12, no. 5, pp. 1221-1250, Jun. 2008.
- [23] M. Winter and R. J. Brodd, "What Are Batteries, Fuel Cells, and Supercapacitors?," *Chem. Rev.*, vol. 104, no. 10, pp. 4245-4270, Oct. 2004.
- [24] Uno, Masatoshi and Koji Tanaka. "Accelerated ageing testing and cycle life prediction of supercapacitors for alternative battery applications." *2011 IEEE 33rd International Telecommunications Energy Conference (INTELEC) (2011)*: 1-6.
- [25] Pei Yulong, A. Cavagnino, S. Vaschetto, Chai Feng and A. Tenconi, "Flywheel energy storage systems for power systems application," *2017 6th International Conference on Clean Electrical Power (ICCEP)*, Santa Margherita Ligure, 2017, pp. 492-501.
- [26] R. H. Byrne, T. A. Nguyen, D. A. Copp, B. R. Chalamala and I. Gyuk, "Energy Management and Optimization Methods for Grid Energy Storage Systems," in *IEEE Access*, vol. 6, pp. 13231-13260, 2018.
- [27] Eurelectri-U. of the E. Industry, "Ancillary Services Unbundling Electricity Products - an Emerging Market," no. February, p. 84, 2004.
- [28] G. Fuchs, B. Lunz, M. Leuthold, and D. U. Sauer, "Technology Overview on Electricity Storage - Overview on the potential and on the deployment perspectives of electric storage technologies," *Inst. Power Electron. Electr. Drives (ISEA), RWTH Aachen Univ.*, no. June, p. 66, 2012.
- [29] V. Calderano, V. Galdi, F. Lamberti, and A. Piccolo, "Co-located storage systems with renewable energy sources for voltage support in distribution networks," in *2015 IEEE Power & Energy Society General Meeting*, 2015, vol. 2015 Septe, pp.1-5.
- [30] I. Beil, A. Allen, A. Tokombayev, and M. Hack, "Considerations when using utility-scale battery storage to black start a gas turbine generator," in *2017 IEEE Power & Energy Society General Meeting*, 2017, vol. 2018-Janua, pp. 1-5.
- [31] Modelo de Organização do Mercado Ibérico de Electricidade. Available: <https://mibel.com/> . [Accessed: 02-10-2019].
- [32] Website ERSE. Available: <https://www.erse.pt/inicio/> [Accessed: 02-10-2019]
- [33] J. C. S. Souza, A. M. Leite da Silva and A. P. Alves da Silva, "Data debugging for real-time power system monitoring based on pattern analysis," in *IEEE Transactions on Power Systems*, vol. 11, no. 3, pp. 1592-1599, Aug. 1996.
- [34] A. M. Leite da Silva, L. C. de Resende, L. A. da Fonseca Manso and V. Miranda, "Composite Reliability Assessment Based on Monte Carlo Simulation and Artificial Neural Networks," in *IEEE Transactions on Power Systems*, vol. 22, no. 3, pp. 1202-1209, Aug. 2007.

58 References

- [35] A. G. Ivakhnenko, "Polynomial Theory of Complex Systems," in *IEEE Transactions on Systems, Man, and Cybernetics*, vol. SMC-1, no. 4, pp. 364-378, Oct. 1971.
- [36] S. Makhoulfi and G. G. Pillai, "Wind speed and wind power forecasting using wavelet denoising-GMDH neural network," *2017 5th International Conference on Electrical Engineering - Boumerdes (ICEE-B)*, Boumerdes, 2017.
- [37] Khosravi, Ali & Machado, Luiz & Nunes, R.. (2018). Time-series prediction of wind speed using machine learning algorithms: A case study Osorio wind farm, Brazil. *Applied Energy*. 224. 10.1016/j.apenergy.2018.05.043.
- [38] L. Bianchi, M. Dorigo, L. M. Gambardella, and W. J. Gutjahr, "A survey on metaheuristics for stochastic combinatorial optimization," *Nat. Comput.*, vol. 8, no. 2, pp. 239-287, 2009.
- [39] J. Kennedy, "Particle Swarm Optimization," in *Encyclopedia of Machine Learning and Data Mining*, vol. 46, no. 10, Boston, MA: Springer US, 2017, pp. 967-972.
- [40] V. Miranda and N. Fonseca, "EPSO - best-of-two-worlds meta-heuristic applied to power system problems," in *Proceedings of the 2002 Congress on Evolutionary Computation. CEC'02 (Cat. No.02TH8600)*, 2002, vol. 2, pp. 1080-1085.
- [41] V. Miranda, H. Keko, and A. Jaramillo, "EPSO: Evolutionary particle swarms," *Stud. Comput. Intell.*, vol. 66, pp. 139-167, 2007.
- [42] V. Miranda and N. Fonseca, "EPSO-evolutionary particle swarm optimization, a new algorithm with applications in power systems," in *IEEE/PES Transmission and Distribution Conference and Exhibition, 2003, vol. 2, pp. 745-750*.
- [43] T. Abreu, "BASSILO," Universidade do Porto, 2019.
- [44] V. Miranda and R. Alves, "Differential Evolutionary Particle Swarm Optimization (DEEPSO): A Successful Hybrid," *2013 BRICS Congress on Computational Intelligence and 11th Brazilian Congress on Computational Intelligence*, Ipojuca, 2013, pp. 368-374.
- [45] Energias de Portugal(EDP), "Perfis de consumo 2019",2018. Available: <https://www.edpdistribuicao.pt/en/node/19436> [Accessed: 19-01-2020].
- [46] R.J. Bessa, A. Trindade, V. Miranda, "Spatial-temporal solar power forecasting for Smart Grids," *IEEE Transactions on Industrial Informatics*, vol. 11, no. 1, pp. 232-241, Feb. 2015.
- [47] Website OMIE. Available: <http://www.omie.es> [Accessed:10-11-2019]
- [48] MATLAB, Introduction - product overview. *The MathWorks*, 2010.
- [49] R.E. Rosenthal. Gams - a user's guide. *GAMS Development Corporation*, 2008
- [50] K. Strunz, E. Abbasi, R. Fletcher, N. Hatziaargyriou, R. Iravani, and G. Joos, TF C6.04.02 : TB 575 -- *Benchmark Systems for Network Integration of Renewable and Distributed Energy Resources*. 2014.